J. Chem. Eng. Data **1987**, *32*, 251-265

Physical and Thermodynamic Properties for Novel C_{14} Unsaturated Aldehydes and C_{16} Saturated Amines

Patrick L. Mills,* Ricky L. Fenton, and George F. Schaefer
Central Research Laboratory, Monsanto Company, St. Louis, Missouri 63167

Various group contribution methods and thermodynamic correlating equations were used to develop physical and thermodynamic properties for 28 branched isomeric C_{14} unsaturated aldehydes and 28 isomeric C_{16} amines derived from these aldehydes, the majority of which represent novel compositions. The particular properties that were derived include normal boiling temperatures, critical constants, vapor pressures, liquid densities, liquid heat capacities, and various ideal gas properties. Vapor pressures, liquid densities, and liquid heat capacities for 2-pentylnonenal, 2-(1,2-dimethylpropyl)-5,6-dimethylheptenal, and *N,N*-dimethyl-2-pentylnonylamine, which represent the least and most highly branched compounds, were experimentally measured and interpreted by using various correlating equations. The experimental results were in good agreement with most of the independently derived properties, which supports the accuracy of the estimation techniques and their utility for engineering applications involving these compounds.

Introduction

Several new approaches have recently been proposed (*1*) for generating low cost detergent hydrophobes that are novel compositions. These approaches couple conventional oxo olefin hydroformylation process technology with condensation–dehydration of the resulting saturated aldehydes via a so-called oxo-aldol synthesis to produce long-chain (e.g., n = 8–20) unsaturated branched aldehydes (enals) as process chemical intermediates. These enal intermediates can then be used to produce additional novel compositions such as long-chain alcohols, amines, amine oxides, and quaternary salts, to name a few, in additional process steps. Of particular interest in this work is development of physical properties for the C_{14} unsaturated aldehydes and C_{16} saturated amines produced by the three oxo-aldol-reductive amination reaction sequences A–C.

$$C_6H_{12} + CO + H_2 \longrightarrow C_6H_{13}CHO \qquad (A)$$

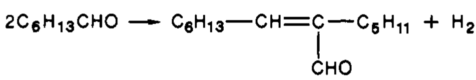

$$2C_6H_{13}CHO \longrightarrow C_6H_{13}{-}CH{=}\underset{\displaystyle CHO}{\underset{|}{C}}{-}C_5H_{11} + H_2O \qquad (B)$$

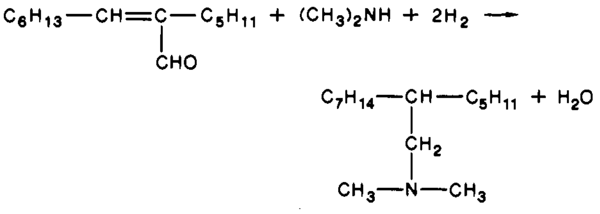

$$C_6H_{13}{-}CH{=}\underset{\displaystyle CHO}{\underset{|}{C}}{-}C_5H_{11} + (CH_3)_2NH + 2H_2 \longrightarrow C_7H_{14}{-}\underset{\displaystyle CH_3{-}N{-}CH_3}{\underset{|}{\underset{\displaystyle CH_2}{\underset{|}{CH}}}}{-}C_5H_{11} + H_2O \qquad (C)$$

When the hydroformylation reaction given by eq A is performed using a mixture of C_6 olefins and octacarbonyldicobalt as the homogeneous catalyst precursor, a mixture of C_7 aldehydes is obtained which can ultimately lead to 28 isomeric C_{14} enals (excluding diastereomers) as potential reaction products in eq B. Reductive amination of these C_{14} enals using dimethylamine and hydrogen can, in principle, lead to 28 isomeric C_{16} saturated amines as shown by eq C. Tables I and II give the names and structures of these C_{14} enals and C_{16} amines, all of which represent novel compositions with the exception of compound 5 in Table I, namely, 2-pentylnonenal.

The principle objective of the work is to provide fundamental physical property and thermodynamic data for the 56 species listed in Tables I and II since these represent novel compounds so that such data are nonexistent. The approach used here involves the application of various group contribution and other thermodynamic correlations to obtain estimates of normal boiling temperatures, critical properties, vapor pressures, liquid densities, liquid heat capacities, and ideal gas properties. Experimental measurements for vapor pressures, liquid densities, and liquid heat capacities are obtained for the least and most highly branched isomers and compared to the group contribution and estimated values. Evidence is provided on this basis that the estimated values of physicochemical properties are usually within acceptable limits of error for engineering applications.

Typical applications in which both the derived and experimental thermodynamic property data should prove useful might include process conceptualization, process flowsheeting calculations, process equipment design and simulation, and various other process and product development applications. In fact, development of a FLOWTRAN simulation for a proposed process involving the above C_{14} enals and C_{16} amines as intermediates was the original motivation for this work.

Experimental Section

***Materials*.** Preparation of 2-pentylnonenal (species 5 in Table I), which is the C_{14} enal having the least branching along the main carbon chain, was performed by aldol condensation of n-heptanal. Methanol was used as a cosolvent to increase the mutual solubility of the n-heptanal and hydroxide ion so that acceptable reaction rates could be obtained. The reactants were used as received from commercial sources without further treatment. In a typical run, 803.7 g (1 L) of methanol and 1037.9 g (1 L) of 1 N aqueous NaOH solution was charged to a 1-gallon autoclave. The autoclave was sealed and pressurized with argon to 200 psig (1378.5 kPa), agitated, and vented to degas the caustic–methanol mixture of dissolved oxygen. After this procedure was repeated several times, 818.3 g (1 L) of n-heptanal was charged to the reactor under an argon purge. The reactor was sealed and the reactor was heated to 483.15 K (110 °C) where reaction was allowed to occur for 2 h. The reactor was cooled down and the product was removed which readily separated into two liquid phases. The lower (caustic–methanol) phase was discarded, and the top (organic product) phase was washed several times with degassed, distilled water to remove traces of methanol. The product was vacuum distilled to remove other trace impurities and the distillate was analyzed by gas chromatography using a Varian 3700 with a 50 ft × 0.020 in. SP 1000 column. The normalized area count was >99% which indicated that high purity was obtained. Positive identification had been previously performed in exploratory experiments using GCMS.

2-(1,2-Dimethylpropyl)-5,6-dimethylheptenal (species 16 in Table I) was selected as the C_{14} enal with the greatest amount of branching and was prepared by aldol condensation of 3,4-dimethylpentanal using the same procedure outlined above. The parent aldehyde was prepared in a 0.3-L autoclave by

0021-9568/87/1732-0251$01.50/0

Table I. Compound Names and Structures for C_{14} Unsaturated Aldehydes from C_7 Aldehyde Condensation

index	compd[a]	structure
1	2-(3-MeBu)-5-MeOctenal	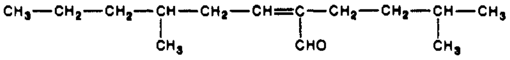 $CH_3-CH_2-CH_2-CH(CH_3)-CH_2-CH{=}C(CHO)-CH_2-CH_2-CH(CH_3)-CH_3$
2	2-(1-MeBu)-5-MeOctenal	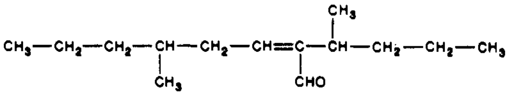 $CH_3-CH_2-CH_2-CH(CH_3)-CH_2-CH{=}C(CHO)-CH(CH_3)-CH_2-CH_2-CH_3$
3	2-Pe-5-MeOctenal	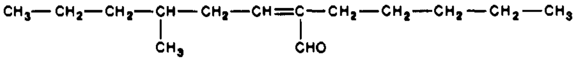 $CH_3-CH_2-CH_2-CH(CH_3)-CH_2-CH{=}C(CHO)-CH_2-CH_2-CH_2-CH_2-CH_3$
4	2-(3-MeBu)-7-MeOctenal	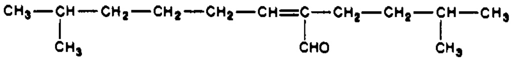 $CH_3-CH(CH_3)-CH_2-CH_2-CH_2-CH{=}C(CHO)-CH_2-CH_2-CH(CH_3)-CH_3$
5	2-PeNonenal	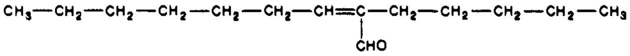 $CH_3-CH_2-CH_2-CH_2-CH_2-CH_2-CH{=}C(CHO)-CH_2-CH_2-CH_2-CH_2-CH_3$
6	2-Pe-7-MeOctenal	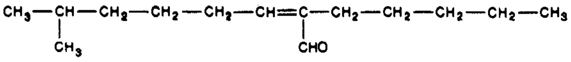 $CH_3-CH(CH_3)-CH_2-CH_2-CH_2-CH{=}C(CHO)-CH_2-CH_2-CH_2-CH_2-CH_3$
7	2-(3-MeBu)-Nonenal	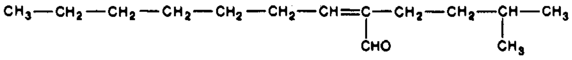 $CH_3-CH_2-CH_2-CH_2-CH_2-CH_2-CH{=}C(CHO)-CH_2-CH_2-CH(CH_3)-CH_3$
8	2-(1-MeBu)-7-MeOctenal	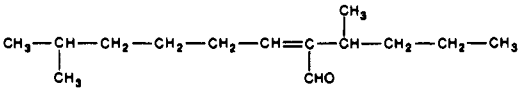 $CH_3-CH(CH_3)-CH_2-CH_2-CH_2-CH{=}C(CHO)-CH(CH_3)-CH_2-CH_2-CH_3$
9	2-Pe-4-MeOctenal	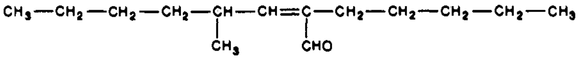 $CH_3-CH_2-CH_2-CH_2-CH(CH_3)-CH{=}C(CHO)-CH_2-CH_2-CH_2-CH_2-CH_3$
10	2-(3-MeBu)-4-MeOctenal	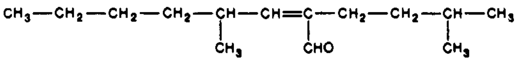 $CH_3-CH_2-CH_2-CH_2-CH(CH_3)-CH{=}C(CHO)-CH_2-CH_2-CH(CH_3)-CH_3$
11	2-(1-MeBu)-Nonenal	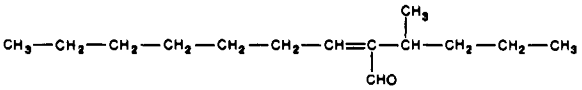 $CH_3-CH_2-CH_2-CH_2-CH_2-CH_2-CH{=}C(CHO)-CH(CH_3)-CH_2-CH_2-CH_3$
12	2-Pe-4-EtHeptenal	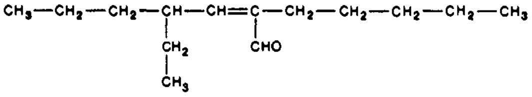 $CH_3-CH_2-CH_2-CH(CH_2-CH_3)-CH{=}C(CHO)-CH_2-CH_2-CH_2-CH_2-CH_3$
13	2-(3-MeBu)-4-EtHeptenal	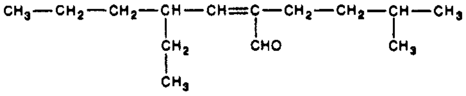 $CH_3-CH_2-CH_2-CH(CH_2-CH_3)-CH{=}C(CHO)-CH_2-CH_2-CH(CH_3)-CH_3$
14	2-(1-MeBu)-4-MeOctenal	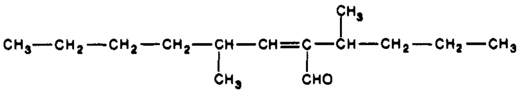 $CH_3-CH_2-CH_2-CH_2-CH(CH_3)-CH{=}C(CHO)-CH(CH_3)-CH_2-CH_2-CH_3$
15	2-(1-MeBu)-4-EtHeptenal	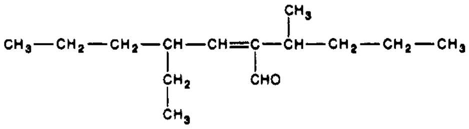 $CH_3-CH_2-CH_2-CH(CH_2-CH_3)-CH{=}C(CHO)-CH(CH_3)-CH_2-CH_2-CH_3$
16	2-(1,2-DiMePr)-5,6-DiMeHeptenal	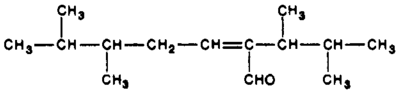 $CH_3-CH(CH_3)-CH(CH_3)-CH_2-CH{=}C(CHO)-CH(CH_3)-CH(CH_3)-CH_3$
17	2-Pe-5,6-DiMeHeptenal	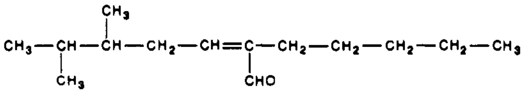 $CH_3-CH(CH_3)-CH(CH_3)-CH_2-CH{=}C(CHO)-CH_2-CH_2-CH_2-CH_2-CH_3$
18	2-(1,2-DiMePr)-Nonenal	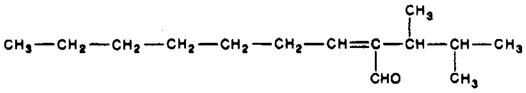 $CH_3-CH_2-CH_2-CH_2-CH_2-CH_2-CH{=}C(CHO)-CH(CH_3)-CH(CH_3)-CH_3$
19	2-(3-MeBu)-5,6-DiMeHeptenal	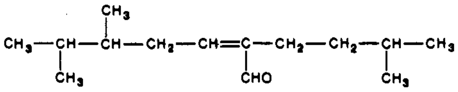 $CH_3-CH(CH_3)-CH(CH_3)-CH_2-CH{=}C(CHO)-CH_2-CH_2-CH(CH_3)-CH_3$
20	2-(1,2-DiMePr)-7-MeOctenal	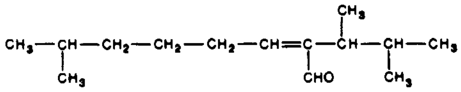 $CH_3-CH(CH_3)-CH_2-CH_2-CH_2-CH{=}C(CHO)-CH(CH_3)-CH(CH_3)-CH_3$

Table I (Continued)

index	compd[a]	structure
21	2-(1,2-DiMePr)-5-MeOctenal	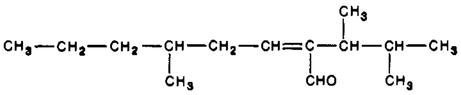 $CH_3-CH_2-CH_2-CH(CH_3)-CH_2-CH=C(CHO)-CH(CH_3)-CH(CH_3)-CH_3$
22	2-(1-MeBu)-5,6-DiHeptenal	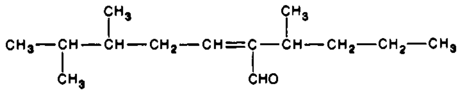 $CH_3-CH(CH_3)-CH(CH_3)-CH_2-CH=C(CHO)-CH(CH_3)-CH_2-CH_2-CH_3$
23	2-(1,2-DiMePr)-4-MeOctenal	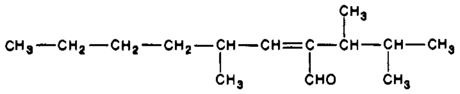 $CH_3-CH_2-CH_2-CH_2-CH(CH_3)-CH=C(CHO)-CH(CH_3)-CH(CH_3)-CH_3$
24	2-(1,2-DiMePr)-4-EtHeptenal	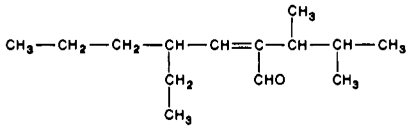 $CH_3-CH_2-CH_2-CH(CH_2CH_3)-CH=C(CHO)-CH(CH_3)-CH(CH_3)-CH_3$
25	2-Pe-4,6-DiMeHeptenal	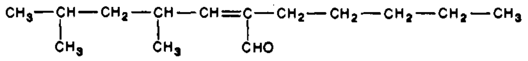 $CH_3-CH(CH_3)-CH_2-CH(CH_3)-CH=C(CHO)-CH_2-CH_2-CH_2-CH_2-CH_3$
26	2-(3-MeBu)-4,6-DiMeHeptenal	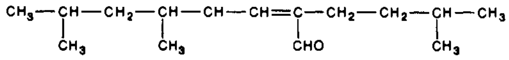 $CH_3-CH(CH_3)-CH_2-CH(CH_3)-CH-CH=C(CHO)-CH_2-CH_2-CH(CH_3)-CH_3$
27	2-(1,2-DiMePr)-4,6-DiMeHeptenal	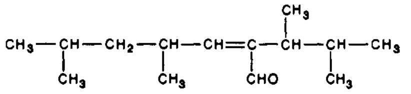 $CH_3-CH(CH_3)-CH_2-CH(CH_3)-CH=C(CHO)-CH(CH_3)-CH(CH_3)-CH_3$
28	2-(1-MeBu)-4,6-DiMeHeptenal	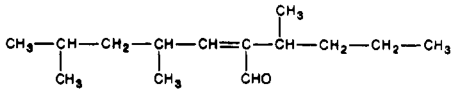 $CH_3-CH(CH_3)-CH_2-CH(CH_3)-CH=C(CHO)-CH(CH_3)-CH_2-CH_2-CH_3$

[a] Abbreviations: Me, methyl; Et, ethyl; Pr, propyl; Bu, butyl; Pe, pentyl.

hydroformylation of 100 g of 2,3-dimethylpentene with 0.75 g of HRhCO[$(C_6H_5)_3P$]$_3$ catalyst precursor and 36 g of $(C_6H_5)_3P$ as promoter at 500 psig (3447 kPa) of 1:1 H_2/CO at 393.15 K (120 °C). The purity of the enal obtained after distillation was >98% as determined by GC.

The C_{16} saturated amine having the least amount of branching is *N*,*N*-dimethyl-2-pentylnonylamine (species 5 in Table II). This was prepared in a 0.3-L autoclave by reacting 123.32 g of 2-pentylnonenal with 30.36 g of dimethylamine in the presence of 1.54 g of Engelhard 5% Pd-on-carbon powder at T = 383.15 K (110 °C) and P = 500 psig (3447 kPa) of hydrogen until no gas uptake was detected (about 4 h). The product was separated from the catalyst by vacuum filtration and distilled. The distillate was analyzed by gas chromatography using a procedure outlined in detail elsewhere (*2*) that is based upon forming the trimethylsilyl oxime derivative of 2-pentylnonenal. This was necessary since the similar boiling points of the C_{14} enal and the C_{16} amine prevented adequate peak resolution when no derivization of the samples was performed. The purity of the C_{16} amine determined by this procedure was found to be nearly 99.9%.

Thermal Stability Measurements. The C_{14} unsaturated aldehydes and C_{16} amine were subjected to thermal stability measurements to determine the upper temperature limit where these materials begin to decompose to gaseous products. A specially designed instrument based upon accelerating rate calorimetry was used for this purpose. In a typical experiment, a sample of the pure aldehyde or amine was placed in a spherical bomb constructed of Hastelloy C in the presence of an inert gas and connected to appropriate temperature and pressure sensors. The sample temperature was then increased to 398.15 K (125 °C) at which point a sequence consisting of a 10-min wait, 20-min search, and 5 K heating was initiated. This was continued until the sample achieved at least a self-heating rate of 0.01 K min^{-1}. The sample was then maintained at an adiabatic state until the self-heating rate dropped below 0.008 K min^{-1}. Alternating operation between the above three-step sequence and the adiabatic modes was continued until either an upper temperature limit of 673.15 K (300 °C) was reached or gas evolution was detected. For 2-pentylnonenal, the initial temperature at which self-heating was detected occurred at 509.15 K (236 °C) while the initial temperature at which gas evolution was observed occurred at 483.15 K (210 °C). For 2-(1,2-dimethylpropyl)-5,6-dimethylheptenal, the corresponding temperatures were 573.15 K (300 °C) and 503.15 K (230 °C), respectively. In the case of *N*,*N*-dimethyl-2-pentylnonylamine, the temperatures were both greater than 573.15 K (300 °C). On the basis of these results, it can be concluded any physical property measurements for these species that are performed in excess of the initial self-heating or gas evolution temperatures may be subject to errors. For some of the physical property data reported below, measurements were made in excess of these temperatures. However, the time required to perform the measurement (for example, vapor pressure) was typically rapid enough that the contribution of decomposition was less than 1% as determined by repeated measurements.

Vapor Pressure Measurements. A Hoover-John-Mellen semimicro ebulliometer with about 0.003 L of sample was used to perform the vapor pressure measurements. Readings were taken at a series of discrete temperatures over a range of 5 Torr, or an initial pressure which corresponded to a boiling point of 323.15 K, to 760 Torr. Pressures were measured with a Texas Instruments fused quartz pressure gauge which has a worst case precision of ±0.04 Torr. Temperatures were measured with a glass-sheathed platinum RTD probe having an accuracy of ±0.02 K. An Omega temperature indicator was used with an accuracy of ±0.1 K. During a series of measurements, the temperature varied from 0.01 to 0.2 K. The accuracy of the measurements was checked by using hexadecane as a reference material and comparing the results to literature values. Comparisons between the experimental and

Table II. Compound Names and Structures for C_{16} Saturated Amines from Reductive Amination of C_{14} Unsaturated Aldehydes

index	compd[a]	structure
1	*N*,*N*-DiMe-2-(3-MeBu)-5-MeOcAm	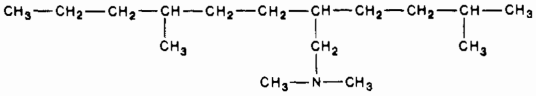
2	*N*,*N*-DiMe-2-(1-MeBu)-5-MeOcAm	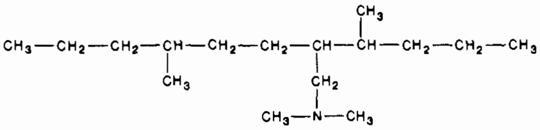
3	*N*,*N*-DiMe-2-Pe-5-MeOcAm	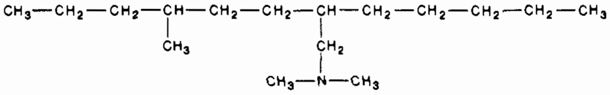
4	*N*,*N*-DiMe-2-(3-MeBu)-7-MeOcAm	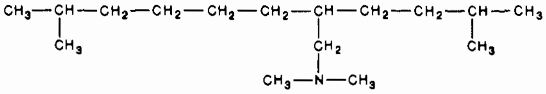
5	*N*,*N*-DiMe-2-PeNyAm	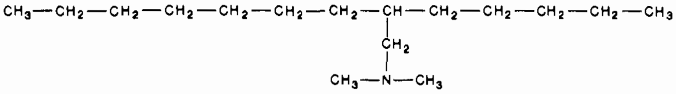
6	*N*,*N*-DiMe-2-Pe-7-MeOcAm	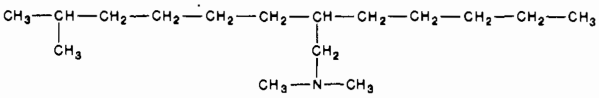
7	*N*,*N*-DiMe-2-(3-MeBu)-NyAm	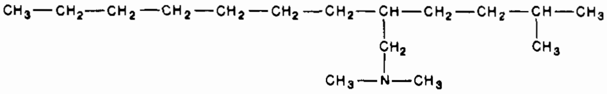
8	*N*,*N*-DiMe-2-(1-MeBu)-7-MeOcAm	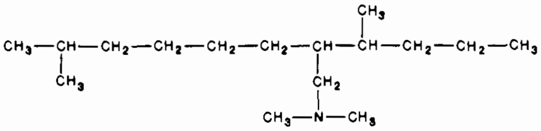
9	*N*,*N*-DiMe-2-Pe-4-MeOcAm	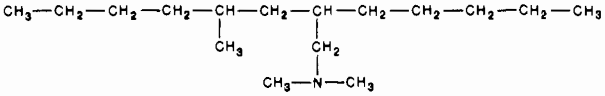
10	*N*,*N*-DiMe-2-(3-MeBu)-4-MeOcAm	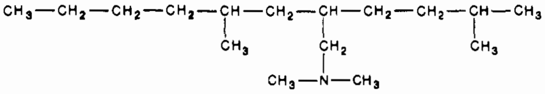
11	*N*,*N*-DiMe-2-(1-MeBu)-NyAm	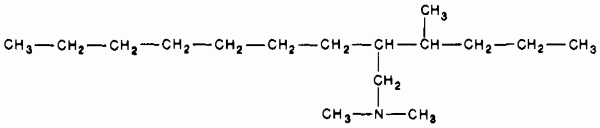
12	*N*,*N*-DiMe-2-Pe-4-EtHpAm	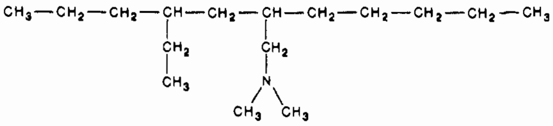
13	*N*,*N*-DiMe-2-(3-MeBu)-4-EtHpAm	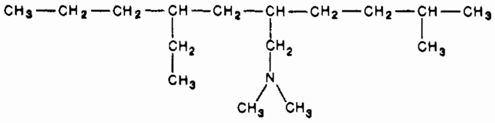
14	*N*,*N*-DiMe-2-(1-MeBu)-4-MeOcAm	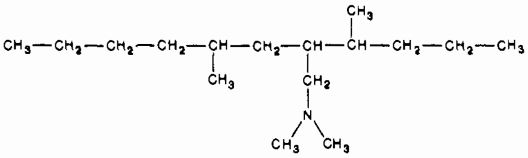
15	*N*,*N*-DiMe-2-(1-MeBu)-4-EtHpAm	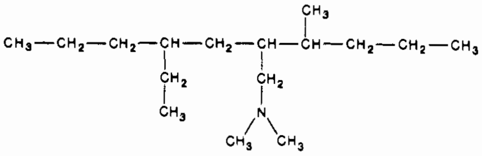

Table II (Continued)

index	compd[a]	structure
16	*N*,*N*-DiMe-2-(1,2-DiMePr)-5,6-DiMeHpAm	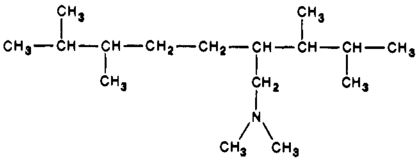
17	*N*,*N*-DiMe-2-Pe-5,6-DiMeHpAm	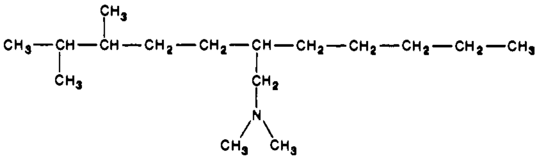
18	*N*,*N*-DiMe-2-(1,2-DiMePr)-NyAm	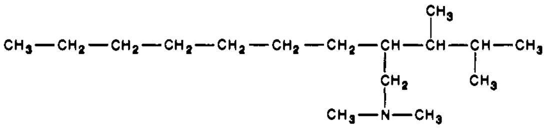
19	*N*,*N*-DiMe-2-(3-MeBu)-5,6-DiMeHpAm	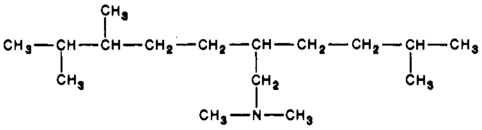
20	*N*,*N*-DiMe-2-(1,2-DiMePr)-7-MeOcAm	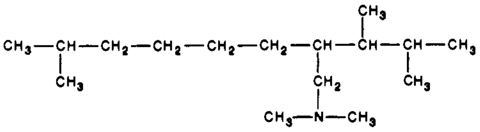
21	*N*,*N*-DiMe-2-(1,2-DiMePr)-5-MeOcAm	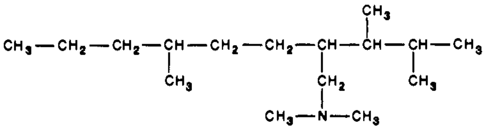
22	*N*,*N*-DiMe-2-(1-MeBu)-5,6-DiMeHpAm	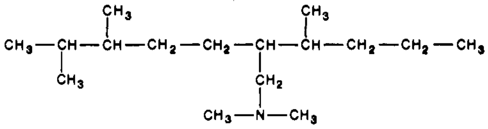
23	*N*,*N*-DiMe-2-(1,2-DiMePr)-4-MeOcAm	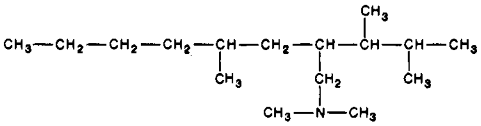
24	*N*,*N*-DiMe-2-(1,2-DiMePr)-4-EtHpAm	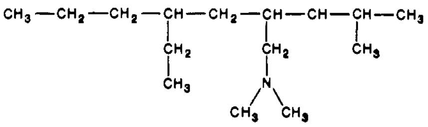
25	*N*,*N*-DiMe-2-Pe-4,5-DiMeHpAm	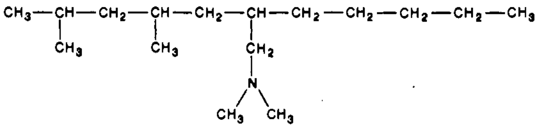
26	*N*,*N*-DiMe-2-(3-MeBu)-4,6-DiMeHpAm	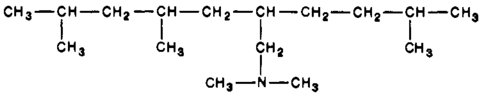
27	*N*,*N*-DiMe-2-(1,2-DiMePr)-4,5-DiMeHpAm	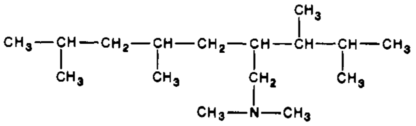
28	*N*,*N*-DiMe-2-(1-MeBu)-4,6-DiMeHpAm	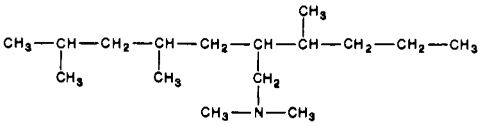

[a] Abbreviations: Me, methyl; Et, ethyl; Pr, propyl; Bu, butyl; Pe, pentyl; Hp, heptyl; Oc, octyl; Ny, nonyl; Am, amine.

Table III. Normal Boiling Temperatures and Critical Constants for C_{14} Unsaturated Aldehydes

compd[a]	T_b, K	T_c, K	P_c, atm	V_c, cm^3 mol^{-1}	Z_c
2-(3-MeBu)-5-MeOctenal	557.589	729.733	17.017	791	0.2248
2-(1-MeBu)-5-MeOctenal	557.589	729.733	17.017	791	0.2248
2-Pe-5-MeOctenal	563.591	734.114	16.853	795	0.2224
2-(3-MeBu)-7-MeOctenal	557.589	729.733	17.017	791	0.2248
2-PeNonenal	569.467	738.413	16.9692	799	0.2201
2-Pe-7-MeOctenal	563.591	734.114	16.853	795	0.2224
2-(3-MeBu)-Nonenal	563.591	734.114	16.853	795	0.2224
2-(1-MeBu)-7-MeOctenal	557.589	729.733	17.017	791	0.2248
2-Pe-4-MeOctenal	563.591	734.114	16.853	795	0.2224
2-(3-MeBu)-4-MeOctenal	557.589	729.733	17.017	791	0.2248
2-(1-MeBu)-Nonenal	563.591	734.114	16.853	795	0.2224
2-Pe-4-EtHeptenal	563.591	734.114	16.853	795	0.2224
2-(3-MeBu)-4-EtHeptenal	557.589	729.733	17.017	791	0.2248
2-(1-MeBu)-4-MeOctenal	557.589	729.733	17.017	791	0.2248
2-(1-MeBu)-4-EtHeptenal	557.589	729.733	17.017	791	0.2248
2-(1,2-DiMePr)-5,6-DiMeHeptenal	554.747	733.323	17.350	783	0.2258
2-Pe-5,6-DiMeHeptenal	562.288	735.882	17.017	791	0.2229
2-(1,2-DiMePr)-Nonenal	562.288	735.882	17.017	791	0.2229
2-(3-MeBu)-5,6-DiMeHeptenal	556.277	731.535	17.182	787	0.2253
2-(1,2-DiMePr)-7-MeOctenal	556.227	731.535	17.182	787	0.2253
2-(1,2-DiMePr)-5-MeOctenal	556.227	731.535	17.182	787	0.2253
2-(1-MeBu)-5,6-DiMeHeptenal	556.277	731.535	17.182	787	0.2253
2-(1,2-DiMePr)-4-MeOctenal	556.227	731.535	17.182	787	0.2253
2-(1,2-DiMePr)-4-EtHeptenal	556.277	731.535	17.182	787	0.2253
2-Pe-4,6-DiMeHeptenal	543.283	711.010	17.017	791	0.2307
2-(3-MeBu)-4,6-DiMeHeptenal	551.463	725.269	17.182	787	0.2272
2-(1,2-DiMePr)-4,6-DiMeHeptenal	550.044	727.106	17.350	783	0.2277
2-(1-MeBu)-4,6-DiMeHeptenal	551.463	725.269	17.182	787	0.2272

[a] Abbreviations: Me, methyl; Et, ethyl; Pr, propyl; Bu, butyl; Pe, pentyl.

literature results are given in Table I of a related paper (*3*). The maximum deviation between these results was 0.86% with a mean deviation of 0.41%. On the basis of these data, the vapor pressure data for the compounds in this work can be expected to have similar errors.

Density Measurements. Density measurements were made over the range 298.15–423.15 K using calibrated stem pycnometers immersed in a thermostated bath whose temperature was measured within ±0.1 K. The estimated error in the density values is ±0.002 g cm^{-3}.

Heat Capacity Measurements. The liquid heat capacity of *N,N*-dimethyl-2-pentylnonylamine was measured over the range 303.15–423.15 K by differential scanning calorimetry using a Perkin-Elmer DSC-2C. The sample was encapsulated in a gold pan under ambient conditions. The heat capacity was calculated by comparison to a sapphire specific heat capacity standard. The accuracy of the instrument was tested by using diphenyl ether as a reference material and performing measurements over the same temperature range. Table II of a related publication (*3*) gives a comparison between the experimental and literature values for the standard. It is shown that the maximum deviation of the errors is 1.65% for the experimental values with a mean deviation of 1.01%. Based on these results, the heat capacity data for the above C_{16} amine can be expected to have similar errors.

Results and Discussion

Normal Boiling Temperatures and Critical Properties. Tables III and IV list values for the normal boiling temperatures and critical properties for each of the C_{14} enals and C_{16} amines given previously in Tables I and II, respectively. The critical temperature T_c for each compound was obtained from the group contribution method of Fedors (*4*), while the critical pressure P_c, critical volume V_c, and the reduced boiling point T_{br} were obtained by using the group contribution method of Lydersen as outlined by Reid et al. (*5*). The normal boiling point T_b was obtained from the estimated values of critical temperature and reduced boiling point using eq 1 The critical compressibility Z_c was obtained from the known values of P_c, V_c, and T_c by using

$$T_b = T_{br}T_c \qquad (1)$$

$$Z_c = \frac{P_cV_c}{RT_c} \qquad (2)$$

Comparisons between the normal boiling temperatures obtained by fitting the vapor pressure data for 2-pentylnonenal (enal having the least branching), 2-(1,2-dimethylpropyl)-5,6-dimethylheptenal (enal having the greatest branching), and *N,N*-dimethyl-2-pentylnonylamine (least branched amine) to those obtained from eq 1, which are based on group contribution methods, are given in Table V. The temperature deviation obtained by using the combination of Fedors' method for T_c and Lydersen's method for T_{br} to obtain T_b is less than 4.5% which is acceptable for engineering purposes. Values of T_b obtained from Watson's method (*6*) have large errors so that application of this latter method to this class of compounds is not recommended. Based upon the results given in Table V, it can be concluded that the estimated values of T_b for the remaining C_{14} enals and C_{16} amines where experimental data is not yet available probably have temperature deviations within similar limits. Generally, the boiling temperature estimates suggest that C_{14} enals and C_{16} amines having a greater number of substitutions along the main carbon chain have lower boiling points than those with a lesser number of substitutions. This trend agrees with other classes of compounds, such as the isomers of the C_6 olefins, so that the above estimated values of T_b have the correct qualitative behavior.

Errors associated with the estimated critical properties given in Tables III and IV cannot be directly assessed since experimental data are not yet available. Maximum errors for T_c, P_c, and V_c are given (*5*) s 5%, 10%, and 10–15%, but these may not be reliable for the high molecular weight compounds enals and amines given here. The group contribution values for aldehydes are based upon experimental measurements for only a few compounds so that the data base is quite meager when compared to that for other classes of compounds such as normal paraffins, for example. By their chemical nature, aldehydes are subject to decomposition at elevated temperature and pressure so that it is unlikely that determination of the true

Table IV. Normal Boiling Temperatures and Critical Constants for C_{16} Saturated Amines

compd[a]	T_b, K	T_c, K	P_c, atm	V_c, cm^3 mol^{-1}	Z_c
N,*N*-DiMe-2-(3-MeBu)-5-MeOcAm	563.784	721.967	14.541	950	0.2332
N,*N*-DiMe-2-(1-MeBu)-5-MeOcAm	568.747	728.322	14.541	950	0.2311
N,*N*-DiMe-2-Pe-5-MeOcAm	569.482	726.495	14.421	954	0.2308
N,*N*-DiMe-2-(3-MeBu)-7-MeOcAm	563.784	721.967	14.541	950	0.2332
N,*N*-DiMe-2-Pe-NyAm	575.045	730.936	14.301	958	0.2284
N,*N*-DiMe-2-Pe-7-MeOcAm	569.482	726.495	14.421	954	0.2308
N,*N*-DiMe-2-(3-MeBu)-NyAm	569.482	726.495	14.421	954	0.2308
N,*N*-DiMe-2-(1-MeBu)-7-MeOcAm	568.747	728.322	14.541	950	0.2311
N,*N*-DiMe-2-Pe-4-MeOcAm	569.482	726.495	14.421	954	0.2308
N,*N*-DiMe-2-(3-MeBu)-4-MeOcAm	563.784	721.967	14.541	950	0.2322
N,*N*-DiMe-2-(1-MeBu)-NyAm	574.369	732.729	14.421	954	0.2288
N,*N*-DiMe-2-Pe-4-EtHpAm	569.482	726.495	14.421	954	0.2308
N,*N*-DiMe-2-(3-MeBu)-4-EtHpAm	563.784	721.967	14.541	950	0.2322
N,*N*-DiMe-2-(1-MeBu)-4-MeOcAm	568.747	728.322	14.541	950	0.2311
N,*N*-DiMe-2-(1-MeBu)-4-EtHpAm	568.747	728.322	14.541	950	0.2311
N,*N*-DiMe-2-(1,2-DiMePr)-5,6-DiMeHpAm	564.523	728.827	14.787	942	0.2329
N,*N*-DiMe-2-Pe-5,6-DiMeHpAm	568.747	728.322	14.541	950	0.2311
N,*N*-DiMe-2-(1,2-DiMePr)-NyAm	571.178	731.436	14.541	950	0.2302
N,*N*-DiMe-2-(3-MeBu)-5,6-DiMeHpAm	562.992	723.830	14.663	946	0.2335
N,*N*-DiMe-2-(1,2-DiMePr)-7-MeOcAm	565.461	727.004	14.663	946	0.2325
N,*N*-DiMe-2-(1,2-DiMePr)-5-MeOcAm	565.461	727.004	14.663	946	0.2325
N,*N*-DiMe-2-(1-MeBu)-5,6-DiMeHpAm	567.896	730.135	14.663	946	0.2315
N,*N*-DiMe-2-(1,2-DiMePr)-4-MeOcAm	565.461	727.004	14.663	946	0.2325
N,*N*-DiMe-2-(1,2-DiMePr)-4EtHpAm	565.461	727.004	14.663	946	0.2325
N,*N*-DiMe-2-Pe-4,6-DiMeHpAm	563.784	721.967	14.541	950	0.2322
N,*N*-DiMe-2-(3-MeBu)-4,6-DiMeHpAm	557.952	717.350	14.663	946	0.2357
N,*N*-DiMe-2-(1,2-DiMePr)-4,6-DiMeHpAm	559.612	722.486	14.787	942	0.2350
N,*N*-DiMe-2-(1-MeBu)-4,6-DiMeHpAm	562.992	723.830	14.663	946	0.2335

[a] Abbreviations: Me, methyl; Et, ethyl; Pr, propyl; Bu, butyl; Pe, pentyl; Hp, heptyl; Oc, octyl; Ny, nonyl; Am, amine.

Table V. Comparison between Experimental and Estimated Normal Boiling Temperatures

compd	T_b, K				
	obsd[a]	est[b]	est[c]	ϵ[d]	ϵ[e]
2-pentynonenal	553.50	569.47	355.86	−2.9	35.7
2-(1,2-DiMePr)-5,6-DiMeHeptenal	534.78	554.75	410.45	−3.7	23.2
N,*N*-DiMe-2-PeNyAm	551.93	575.05	405.75	−4.2	26.5

[a] From Antoine eq at $P = 1$ atm. [b] From eq 1. [c] From Watson's method (*6*). [d] ϵ = temperature deviation = $100(T_{b,exptl} - T_{b,est})/T_{b,exptl}$ with $T_{b,est}$ from *b*. [e] Same as *d* except $T_{b,est}$ from *c*.

Table VI. Vapor Pressures of 2-Pentylnonenal

obsd		ϵ,[a] %		
T, K	*P*, kPa	Miller eq	Antoine eq	RPM eq
384.51	0.276	0.01	0.15	51.54
402.41	0.692	0.04	−0.09	43.34
416.68	1.344	0.06	−0.09	36.99
432.87	2.668	−0.22	−0.29	29.97
450.73	5.326	−0.01	0.02	23.20
450.85	5.346	−0.08	−0.05	23.11
470.61	10.658	0.12	0.22	16.55
492.64	21.340	0.75	0.84	10.89
493.06	21.342	−0.48	−0.38	9.69
515.36	40.018	0.08	0.11	5.31
535.85	66.727	−0.62	−0.66	1.31
553.32	101.164	0.33	0.27	0.26

	Miller eq	Antoine eq	RPM eq
mean dev[b]	0.23	0.26	21.01
max dev[a]	0.75	0.84	51.54

[a] ϵ = pressure deviation = $100(P_{exptl} - P_{cald})/P_{exptl}$. [b] $100\,\sum_i(|P_{exptl} - P_{calcd}|/P_{exptl})_i/n$.

critical point will be possible using available experimental methods. For this reason, alternate methods for assessment of the critical point, such as those based upon extrapolation of vapor pressure data, are necessary. Values for the critical pressure, critical temperature, and the acentric factor obtained by application of this approach are compared to the group contribution based values in a later section.

Table VII. Vapor Pressures of 2-(1,2-Dimethylpropyl)-5,6-dimethylheptenal

obsd		ϵ,[a] %		
T, K	*P*, kPa	Miller eq	Antoine eq	RPM
367.63	0.28	0.26	0.55	39.61
384.79	0.69	−0.39	−0.63	32.60
398.65	1.34	0.18	−0.13	28.02
414.62	2.67	−0.03	−0.24	22.60
414.88	2.68	−0.65	−0.87	22.03
424.66	4.00	0.26	0.15	19.78
438.28	6.67	0.26	0.30	16.01
458.64	13.36	0.49	0.68	11.31
481.18	26.34	0.06	0.27	6.51
481.25	26.37	−0.03	0.18	6.41
496.48	39.94	−0.32	−0.20	3.70
516.92	66.64	−0.52	−0.65	0.86
534.67	101.10	0.42	0.01	0.03

	Miller eq	Antoine eq	RPM eq
mean dev[b]	0.30	0.37	16.11
max dev[a]	−0.65	−0.87	39.61

[a] ϵ = pressure deviation = $100(P_{extl} - P_{calcd})/P_{exptl}$. [b] $100\sum_i(|P_{exptl} - P_{calcd}|/P_{exptl})_i/n$.

Vapor Pressures. The vapor pressure data for each compound given in Table V are presented in Tables VI–VIII. Included also are the relative errors obtained when the Miller (*7*), Antoine (*8*), and Riedel-Plank-Miller (*9*) vapor pressure equations were used to interpret the results. The particular forms of these equations that were used are given below.

Miller equation

$$\ln P = A_m + B_m/T + C_mT + D_mT^2 \qquad (3)$$

Antoine equation

$$\ln P = A_a + \frac{B_a}{T + C_a} \qquad (4)$$

Riedel-Plank-Miller (RPM) equation

$$\ln \frac{P}{P_c} = -\frac{G}{T_r}[1 - T_r^2 + k(3 + T_r)(1 - T_r)^3] \qquad (5)$$

Table VIII. Vapor Pressures of *N,N*-Dimethyl-2-pentylnonylamine

obsd		ϵ,[a] %		
T, K	P, kPa	Miller eq	Antoine eq	RPM eq
401.28	0.67	−0.09	0.19	50.26
415.32	1.32	−0.00	−0.14	44.10
415.48	1.33	0.27	0.13	44.18
431.44	2.66	−0.21	−0.45	37.03
449.17	5.36	−0.02	−0.15	29.89
468.69	10.68	0.01	0.06	22.55
468.71	10.68	0.00	0.06	22.54
490.74	21.38	0.13	0.32	15.24
513.26	40.00	−0.08	0.08	8.53
533.66	66.68	−0.02	−0.01	3.59
551.98	101.23	0.02	−0.20	−0.21

	Miller eq	Antoine eq	RPM eq
mean dev[b]	0.08	0.16	25.29
max dev[a]	0.27	−0.48	50.26

[a] ϵ = pressure deviation = $100(P_{\text{exptl}} - P_{\text{calcd}})/P_{\text{exptl}}$. [b] $100\sum_i(|P_{\text{exptl}} - P_{\text{calcd}}|/P_{\text{exptl}})_i/n$.

The constants in the Miller equation were determined by linear regression, while the constants in the Antoine equation were obtained by nonlinear regression. Initial estimates for the Antoine constants A_a, B_a, and C_a were determined by linear regressions using the following linearized form of eq 4

$$T \ln P = A_a T + D_a - C_a \ln P \tag{6}$$

where

$$D_a = A_a C_a - B_a \tag{7}$$

The constants G and k in the RPM equation were determined from the following equations (*5*, *9*) which require values for the normal boiling temperature T_b and critical constants P_c and T_c

$$h = T_{br}\frac{\ln P_c}{1 - T_{br}} \tag{8}$$

$$G = 0.4835 + 0.4605h \tag{9}$$

$$k = \frac{h/G - (1 + T_{br})}{(3 + T_{br})(1 - T_{br})^2} \tag{10}$$

The utility of the RPM equation is that evaluation of the vapor pressure P for a given temperature T only requires the above three fundamental pure-component constants. This is particularly useful when experimental vapor pressure data are not available such as that encountered with novel compounds. Values of the constants for all three equations are tabulated in Table IX for the compounds listed in Table VI–VIII.

The mean error and the root mean square square deviations of pressure given in Tables VI–IX increase in the order of Miller equation, Antoine equations, and RPM equation. The Miller equation gives errors that are slightly less than the Antoine equation which is not surprising since it has an additional parameter. The RPM equation gives errors that are 2 orders of magnitude greater than either the Miller or Antoine equation. The pressure deviations produced by this equation are greatest at the lowest temperature and show a systematic decrease in deviation as the normal boiling temperature is approached. This equation is apparently either sensitive to errors in the estimated values for T_b, T_c, and P_c, or does not apply well to this class of compounds. This aspect is considered in more detail below.

***Vapor Pressure Data Extrapolation*.** Methods for extrapolation of the vapor pressure data to the critical point were also briefly studied. The primary objective here was to obtain independent values for the critical pressure and critical temperature of comparison to the Lydersen group contribution values given earlier in Tables III and IV.

As shown earlier in Tables VI–VIII, the predicted values for the vapor pressures obtained from the RPM equation produced errors that were 1–2 orders of magnitude greater than those produced by the Miller and Antoine equations when compared to the experimental data. Since the constants in the RPM equation defined by eq 8–10 are derived by using the normal boiling temperature, critical pressure, and critical temperature, the predictions will be sensitive to the particular values used for these parameters. The normal boiling temperature was obtained from the experimental vapor pressure data which suggests that the group contribution values for the critical pressure and critical temperature need to the modified to give reasonable agreement in the experimental range.

The above method of adjusting the critical constants in a long-range vapor pressure equation using limited data represents an application of unconstrained extrapolation. It was used by Ambrose (*10*) to fit vapor pressure data for various compounds using three different correlating equations. Alternate methods for identifying critical constants and the acentric factor include the method of constrained extrapolation (*11*) and methods that are based upon fitting vapor pressure data to equations derived from the principle of corresponding states (*12*, *13*). Ambrose and Patel (*12*) have shown that application of the method of constrained extrapolation to Wagner's vapor pressure equation (*14*, *15*) produces errors between the experimental and predicted values for the critical pressure that are nearly the same as the errors produced by a corresponding-states equation that uses two reference fluids. Since the implementation of this latter approach is more straightforward than the method of constrained extrapolation, it was selected as one of the alternate methods. To provide still another method, the Lee–Kesler vapor pressure equation (*13*) was also selected to

Table IX. Miller, Antoine, and Riedel–Plank–Miller Vapor Pressure Equation Constants

compd	Miller const	Antoine const	RPM const
2-pentylnonenal	$A_m = 0.364005 \times 10^2$ $B_m = -0.107662 \times 10^5$ $C_m = -0.318317 \times 10^{-1}$ $D_m = 0.172572 \times 10^{-4}$	$A_a = 0.151603 \times 10^2$ $B_a = -0.496110 \times 10^4$ $C_a = -0.8291 \times 10^2$	$h = 0.948830 \times 10^1$ $G = 0.485286 \times 10^1$ $k = 0.932016$
prms[a]	0.34	0.36	26.44
2-(1,2-DiMePr)-5,6-DiMeHeptenal	$A_m = 0.335018 \times 10^2$ $B_m = -0.978799 \times 10^4$ $C_m = -0.273793 \times 10^{-1}$ $D_m = 0.141870 \times 10^{-4}$	$A_a = 0.146373 \times 10^2$ $B_a = -0.452210 \times 10^4$ $C_a = -0.834200 \times 10^2$	$h = 0.886467 \times 10^1$ $G = 0.456568 \times 10^1$ $k = 0.830957$
prms[a]	0.35	0.45	20.16
N,N-DiMe-2-PeNyAm	$A_m = 0.399782 \times 10^2$ $B_m = -0.115356 \times 10^5$ $C_m = -0.363506 \times 10^{-4}$ $D_m = 0.183877 \times 10^{-4}$	$A_a = 0.143273 \times 10^2$ $B_a = -0.429390 \times 10^4$ $C_a = -0.109670 \times 10^3$	$h = 0.981363 \times 10^1$ $G = 0.500268 \times 10^1$ $k = 0.101573 \times 10^1$
prms[a]	0.12	0.20	30.18

[a] Percent root mean square deviation defined by $100[\sum_i((P_{\text{exptl}} - P_{\text{calcd}})/P_{\text{exptl}})_i^2/n]^{1/2}$.

Table X. Comparison between Critical Properties and Acentric Factors for 2-Pentylnonenal

obsd		ϵ,[a] %		
T, K	P, kPa	two-fluid corresp-states eq	Lee–Kesler eq	RPM eq
384.51	0.276	3.34	−0.41	−0.40
402.41	0.692	0.55	0.17	0.17
416.68	1.344	−0.75	0.36	0.35
432.87	2.668	−1.77	0.10	0.09
450.73	5.326	−1.76	0.17	0.16
450.85	5.346	−1.83	0.10	0.09
470.61	10.658	−1.32	0.06	0.06
492.64	21.340	0.06	0.44	0.45
493.06	21.342	−1.16	−0.79	−0.78
515.36	40.018	0.47	−0.36	−0.33
535.85	66.727	0.96	−0.98	−0.96
553.32	101.164	3.04	0.24	0.24

	Lydersen's method	two-fluid corresp-states eq	Lee-Kesler eq	RPM eq
mean dev[b]		1.42	0.35	0.31
max dev[a]		3.34	−0.98	−0.96
P_c, atm	16.69	13.98	39.52	47.60
T_c, K	738.41	716.34	810.95	825.36
ω		0.7151	0.4644	0.4556

[a] ϵ = pressure deviation = $100(P_{\text{exptl}} - P_{\text{calcd}})/P_{\text{exptl}}$. [b] $100\sum_i(|P_{\text{exptl}} - P_{\text{calcd}}|/P_{\text{exptl}})_i/n$.

Table XI. Comparison between Critical Properties and Acentric Factors for 2-(1,2-Dimethylpropyl)-5,6-dimethylheptenal

obsd		ϵ,[a] %		
T, K	P, kPa	two-fluid corresp-states eq	Lee–Kesler eq	RPM eq
367.63	0.281	3.38	−0.04	−0.04
384.79	0.688	−0.09	−0.36	−0.35
398.65	1.337	−0.53	0.34	0.34
414.62	2.668	−1.35	0.17	0.16
414.88	2.680	−1.99	−0.46	−0.47
424.66	4.002	−1.17	0.42	0.41
438.28	6.666	−1.07	0.35	0.34
458.64	13.360	−0.38	0.42	0.42
481.18	26.342	−0.06	−0.19	−0.17
481.25	26.370	−0.15	−0.29	−0.27
496.48	39.945	0.12	−0.68	−0.65
516.92	66.639	0.70	−0.94	−0.92
534.67	101.101	2.30	0.02	0.02

	Lydersen's method	two-fluid corresp-states eq	Lee–Kesler eq	RPM eq
mean dev[b]		1.02	0.36	0.35
max dev[a]		3.38	−0.94	−0.92
P_c, atm	17.35	12.472	24.63	32.08
T_c, K	733.32	691.43	748.98	772.07
ω		0.6475	0.4942	0.4528

[a] ϵ = pressure deviation = $100(P_{\text{exptl}} - P_{\text{calcd}})/P_{\text{exptl}}$. [b] $100\sum_i(|P_{\text{exptl}} - P_{\text{calcd}}|/P_{\text{exptl}})_i/n$.

Table XII. Comparison between Critical Properties and Acentric Factors for *N*,*N*-Dimethyl-2-pentylnonylamine

obsd		ϵ,[a] %		
T, K	P, kPa	two-fluid corresp-states eq	Lee–Kesler eq	RPM eq
401.28	0.673	0.69	−0.17	−0.23
415.32	1.320	−0.03	0.02	0.03
415.48	1.333	0.24	0.29	0.30
431.44	2.660	−0.62	−0.15	−0.11
449.17	5.356	−0.47	0.04	0.07
468.69	10.675	−0.27	0.02	0.03
468.71	10.682	−0.28	0.02	0.03
490.74	21.381	0.10	0.07	0.46
513.26	39.999	0.08	−0.22	−0.26
533.66	66.676	0.24	−0.20	−0.24
551.98	101.232	0.32	−0.20	−0.20

	Lydersen's method	two-fluid corresp-states eq	Lee–Kesler eq	RPM eq
mean dev[b]		0.30	0.13	0.18
max dev[a]		0.69	0.29	0.46
P_c, atm	14.30	14.588	11.50	20.89
T_c, atm	30.94	714.74	697.25	749.52
ω		0.7211	0.7711	0.5956

[a] ϵ = pressure deviation = $100(P_{\text{exptl}} - P_{\text{calcd}})/P_{\text{exptl}}$. [b] $100\sum_i(|P_{\text{exptl}} - P_{\text{calcd}}|/P_{\text{exptl}})_i/n$.

provide a third comparison. The equation forms for these equations are given below for reference:

Two-fluid corresponding-states equation

$$\ln P_r = \ln P_{r,1} + (\ln P_{r,2} - \ln P_{r,1})(\omega - \omega_1)/(\omega_2 - \omega_1) \tag{11}$$

Lee–Kesler corresponding-states equation

$$\ln P_r = f^{(0)}(T_r) + \omega f^{(1)}(T_r) \tag{12}$$

where

$$f^{(0)}(T_r) = 5.92714 - 6.09648/T_r - 1.28862 \ln T_r + 0.169341 T_r^6 \tag{13}$$

$$f^{(1)}(T_r) = 15.2518 - 15.6875/T_r - 13.4721 \ln T_r + 0.43577 T_r^6 \tag{14}$$

The acentric factor that appears in eq 11 and 12 is defined by

$$\omega = -\frac{\ln P_r(T_r{=}0.7)}{\ln 10} - 1 \tag{15}$$

The subscripts 1 and 2 that appear in eq 11 refer to the reduced pressures and the acentric factors for the two reference fluids. Equation 11 has the form of a linear interpolation formula so that good vapor pressure predictions for the pure component of interest can be expected when the reference lines are on either side of the expected one for this specie.

The unknown parameters P_c, T_c, and ω in the above equations were obtained by minimizing the following objective function

$$\phi = \sum_{i=1}^{n} [w_i(\ln P_{i,\text{exptl}} - \ln P_{i,\text{obsd}})^2] \tag{16}$$

where the subscript exptl denotes the experimental values of vapor pressure and obsd denotes the calculated values obtained from either the RPM equation given by eq 5 or the corresponding-states equations set forth by eq 11 and 12. In the case of the RPM equation and the Lee–Kesler equation, a search method based upon Marquardt's method (*16*) was used to identify P_c and T_c which were then used to evaluate the acentric factor from eq 15. The unknown parameters $\ln P_c$ and ω were determined from the two-fluid equation by linear least squares. The unknown critical temperature was then obtained from eq 15 by using the Antoine equation to represent the vapor pressure. When this vapor pressure equation is used, the following explicit expression for T_c can be derived

$$T_c = \frac{1}{0.7}\left[\frac{B_a}{\ln P_c - A_a - (1 + \omega)\ln 10} - C_a\right] \tag{17}$$

Equation 17 is valid as long as the vapor pressure data are adequately correlated by the Antoine equation at T_r = 0.7. Alternately, an iterative solution of eq 15 for T_c can be performed where $\ln P_r$ is calculated from eq 11.

Tables X–XII give a comparison of the critical pressures, critical temperatures, and acentric factors that were obtained when the methods described above were applied to the vapor pressure data presented earlier in Tables VI and VII. Included also is a comparison of the percent relative errors between the experimental and predicted values for the vapor pressures. The results for the RPM equation show that the errors have been significantly reduced which can be seen by comparing the last column in Tables VI and VII with the last column in Tables X–XII. Values for the critical pressure and critical temperature that produce these lower errors and yield a good fit over the experimental range are greater than those predicted by Lydersen's group contribution method. The greatest differences are seen to occur in the values for the critical pressure where ratios of the fitted values for P_c to Lydersen's values are between 1.5 and 3. Since the fitted values for P_c and T_c may not necessarily satisfy the generalized constraints set forth by Ambrose et al. (*11*), these values should be viewed as being correlating parameters that might be subject to modification when additional data becomes available.

The errors between the experimental and predicted values of vapor pressure produced by the Lee–Kesler equation are in either exact or close agreement with those derived from the RPM equation. Despite this level of agreement, the fitted values for P_c, T_c, and ω for both methods are noticeably different. Since the functions defined by eq 13 and 14 are based upon fluids whose acentric factors correspond to $\omega = 0$ and $\omega \approx 0.4$, application of the Lee–Kesler equation to fluids having $\omega > 0.4$ represents an extrapolation since the fitted values for the acentric factor are greater than 0.45. With the exception of the amine, the fitted values for P_c and T_c for the two enals in Tables X and XI are greater than those derived from Lydersen's method. The results for the C_{16} amine in Table XII show that the fitted values for P_c and T_c obtained from the Lee–Kesler equation are slightly less than those predicted by Lydersen's method. In this case, however, the apparent value for the acentric factor is $\omega = 0.771$ which represents a significant extrapolation from $\omega \simeq 0.4$.

The results for the two-fluid corresponding-states equation are given in column three of Tables X–XII. For the C_{14} enals, 1-tetradecene ($P_c = 15.4$ atm, $T_c = 689$ K, $\omega = 0.644$), *n*-octane ($P_c = 11.2$ atm, $T_c = 717$ K, $\omega = 0.807$), and *n*-hexadecane ($P_c = 14$ atm, $T_c = 717$ K, $\omega = 0.742$) were chosen as the reference fluids. The above data and vapor pressure equation constants needed to evaluate eq 11 for these reference fluids were obtained from standard sources (*6*). Other C_{14}–C_{18} normal paraffins, olefins, and alcohols were used as reference fluids also, but only slight differences from the mean and maximum deviations were noted when compared to the ones given in Tables X–XII. Although the errors associated with the two-fluid equation are larger than those associated with the Lee–Kesler equation and RPM equation, the derived values for P_c and T_c are in closer agreement with those derived from Lydersen's method. In addition, values for the acentric factor between 0.648 and 0.721 are obtained which are in the expected range for species having a similar type and structure as these unsaturated aldehydes and amines. The results obtained with the two-fluid equation suggest that the derived values for critical properties obtained from Lydersen's method are reasonable first estimates which are in contrast to the comparisons made above for the RPM and the Lee–Kesler equations. Additional high-quality vapor pressure data that cover a broader temperature range where the aldehydes and amines are known to be stable are needed so that the various extrapolation methods can be more closely examined in future work.

Table XIII. Density of 2-Pentylnonenal

obsd		ϵ,[d] %		
T, K	ρ, g cm^{-3}	Yen–Woods[a]	Yen–Woods[b]	empirical[c]
298.15	0.846	−1.43	0.0	0.01
323.15	0.827	−1.93	−0.49	−0.04
348.10	0.809	−2.28	−0.83	0.04
373.10	0.790	−2.70	−1.25	−0.01
398.40	0.771	−3.05	−1.60	−0.03
423.10	0.753	−3.26	−1.80	0.02

	Yen–Woods[a]	Yen–Woods[b]	empirical[c]
mean dev[e]	2.44	0.995	0.025
max dev[d]	−3.26	−1.80	−0.04

[a] From eq 18. [b] From eq 19 with $T_{ref} = 298.15$ K. [c] From eq 20. [d] ϵ = density deviation = $100(\rho_{exptl} - \rho_{calcd})/\rho_{exptl}$. [e] $100\sum_i(|\rho_{exptl} - \rho_{calcd}|)\rho_{exptl})_i/n$.

Table XIV. Density of 2-(1,2-Dimethylpropyl)-5,6-dimethylheptenal

obsd		ϵ,[d] %		
T, K	ρ, g cm^{-3}	Yen–Woods[a]	Yen–Woods[b]	empirical[c]
298.15	0.860	−1.79	0.0	−0.02
323.16	0.842	−2.12	−0.33	0.06
347.64	0.823	−2.57	−0.77	−0.02
373.10	0.804	−2.91	−1.10	−0.01
398.20	0.785	−3.22	−1.40	−0.04
423.05	0.767	−3.34	−1.53	0.04

	Yen–Woods[a]	Yen–Woods[b]	empirical[c]
mean dev[e]	2.66	0.855	0.032
max dev[d]	−3.34	−1.53	0.06

[a] From eq 18. [b] From eq 19 with $T_{ref} = 298.15$ K. [c] From eq 20. [d] ϵ = density deviation = $100(\rho_{exptl} - \rho_{calcd})/\rho_{exptl}$. [e] $100\sum_i(|\rho_{exptl} - \rho_{calcd}|/\rho_{exptl})_i/n$.

Table XV. Density of *N*,*N*-Dimethyl-2-pentylnonylamine

obsd		ϵ,[d] %		
T, K	ρ, g cm^{-3}	Yen–Woods[a]	Yen–Woods[b]	empirical[c]
298.15	0.792	−3.63	0.0	−0.04
323.20	0.774	−4.15	−0.5	−0.01
348.10	0.756	−4.65	−0.98	0.003
373.10	0.739	−4.96	−1.28	0.16
398.20	0.719	−5.63	−1.93	−0.07
423.25	0.701	−5.95	−2.24	−0.04

	Yen–Woods[a]	Yen–Woods[b]	empirical[c]
mean dev[e]	4.83	1.155	0.054
max dev[d]	−5.95	−2.24	0.16

[a] From eq 18. [b] From eq 19 with $T_{ref} = 298.15$ K. [c] From eq 20. [d] ϵ = density deviation = $100(\rho_{exptl} - \rho_{calcd})/\rho_{exptl}$. [e] $100\sum_i(|\rho_{exptl} - \rho_{calcd}|/\rho_{exptl})_i/n$.

Liquid Densities. The liquid density data for each compound given in Table V are presented in Tables XIII–XV along with the relative errors obtained when the Yen–Woods (*17*) equation and an empirical equation form were used to interpret the results. The Yen–Woods equation assumes the following form for a saturated liquid when a liquid density value at a reference temperature is not available:

$$\rho_s = \rho_c[1 + \sum_{j=0}^{4} K_j(1 - T_r)^{j/3}] \qquad (18)$$

If a reference density value is available, then the dependence on ρ_c can be avoided by applying eq 18 at both the reference and desired temperature to obtain the following modified form

$$\rho_s = \rho_{ref}\frac{\sum_{j=0}^{4} K_j(1 - T_r)^{j/3}}{\sum_{j=0}^{4} K_j(1 - T_{r,ref})^{j/3}} \qquad (19)$$

The constants K_j in eq 19 are polynomial functions of the critical compressibility Z_c and are given elsewhere (*5*, *17*). Correction

Table XVI. Yen–Woods and Empirical Liquid Density Equation Constants

compd	Yen–Woods[a]	Yen–Woods[b]	empirical[c]
2-pentylnonenal	$b_0 = 0.263283$	$b_0 = 0.259564$	$A = 0.106807 \times 10^1$
	$b_1 = 0.507156$	$b_1 = 0.499992$	$B = -0.745071 \times 10^{-3}$
	$b_2 = 0.218385$	$b_2 = 0.215300$	
	$b_3 = 0.0$	$b_3 = 0.0$	
	$b_4 = 0.2564681 \times 10^{-1}$	$b_4 = 0.260942 \times 10^{-1}$	
prms[d]	0.02522	0.01177	0.00027
2-(1,2-DiMePr)-5,6-DiMeHeptenal	$b_0 = 0.268663$	$b_0 = 0.263944$	$A = 0.108337 \times 10^1$
	$b_1 = 0.517086$	$b_1 = 0.508004$	$B = -0.748501 \times 10^{-3}$
	$b_2 = 0.229334$	$b_2 = 0.225306$	
	$b_3 = 0.0$	$b_3 = 0.0$	
	$b_4 = 0.205229 \times 10^{-1}$	$b_4 = 0.201624 \times 10^{-1}$	
prms[d]	0.02715	0.01018	0.00036
N,N-DiMe-2-PeNyAm	$b_0 = 0.252050$	$b_0 = 0.243214$	$A = 0.100925 \times 10^1$
	$b_1 = 0.484716$	$b_1 = 0.467723$	$B = -0.727596 \times 10^{-3}$
	$b_2 = 0.217172$	$b_2 = 0.209558$	
	$b_3 = 0.0$	$b_3 = 0.0$	
	$b_4 = 0.172347 \times 10^{-1}$	$b_4 = 0.166305 \times 10^{-1}$	
prms[d]	0.04895	0.01386	0.00076

[a] From eq 20 with ρ_c estimated from Lydersen's method. [b] From eq 20 with ρ_c obtained from eq 22. [c] From eq 20. [d] Percent root mean square deviation defined by $100[\sum_i(\rho_{\text{exptl}} - \rho_{\text{calcd}})/\rho_{\text{exptl}})_i^2/n]^{1/2}$.

terms that account for the effect of pressure on the liquid density are also available (*5*, *17*), but their contribution to the saturated values predicted from eq 18 and 19 was found to be negligible for this work.

The simplest empirical equation form which gave a satisfactory representation of the density data over the temperature range investigated was the linear equation

$$\rho_s = A + BT \qquad (20)$$

where A and B are empirical constants for a given compound as determined by least squares and T is the temperature. Inspection of the results given in Tables XIII–XV shows that eq 20 gives the lowest relative error when compared to those based upon the Yen–Woods equation. Between the two forms of the Yen–Woods equation that were tested, the one based upon a reference density point as expressed by eq 19 had the lowest maximum deviation and provided predictions with a mean deviation of less than 1.6% over the indicated temperature range. Errors associated with the form given by eq 18 were typically within 5% of the experimental values which is quite satisfactory for engineering purposes. Application of this equation to the remaining compounds where a reference density is not available might be expected to have errors within the same order of magnitude.

Values for both the Yen–Woods and empirical liquid density equation constants for each compound are given in Table XVI. For the Yens–Woods equation, the various constant terms that appear in eq 18 and 19 can be lumped together to give the simplified form

$$\rho_s = \sum_{j=0}^{4} b_j(1 - T_r)^{j/3} \qquad (21)$$

where

$$b_j = \rho_c K_j \quad \text{for } j = 0, 1, ..., 4$$

with $K_0 = 1$. In the case of eq 18, the critical density ρ_c was obtained from Lydersen's group contribution method (*5*), while the value of ρ_c used in eq 19 was based upon the specified experimental reference temperature–density data pair derived from eq 18 which can be given as

$$\rho_c = \rho_{s,\text{ref}}[1 + \sum_{j=0}^{4} K_j(1 - T_{r,\text{ref}})^{j/3}]^{-1} \qquad (22)$$

Ideal Gas Thermodynamic Properties. Tables XVII and XVIII contain ideal gas enthalpy of formation $\Delta H_f°$, entropy $S°_{298}$, entropy of formation $\Delta S_f°$, Gibbs free energy of formation $\Delta G_f°$, and heat capacity $C_p°$ at various temperatures for each of the C_{14} enals and C_{16} amines. These were developed by using Benson's group contribution method (*18*, *19*) using the various additive values outlined by Reid et al. (*5*). Correction terms to the ideal gas entropy $S°_{298}$ for symmetry, isomers, and alkane gauche interactions were also included. Tables I and II in the supplementary material contain the specific input data used to evaluate these properties for each compound. The entropy of formation $\Delta S_f°$ was obtained from the derived values of $S°_{298}$ for each compound and the $S°_{298}$ values for the elements given in Stull et al. (*20*) using the elemental synthesis reaction. Values for the ideal gas free energy of formation were calculated from the estimated values of $\Delta H_f°$ and $\Delta S_f°$ by using the following thermodynamic relationship at T = 298.15 K.

$$\Delta G_f° = \Delta H_f° - T\Delta S_f° \qquad (23)$$

Generally, the $\Delta H_f°$ values for the C_{14} enals range between −74.84 and −79.65 kcal mol^{-1} corresponding to 2-(3-MeBu)-7-MeOctenal and 2-(3-MeBu)-4,6-DiMeHeptenal, respectively. The corresponding C_{16} amines have $\Delta H_f°$ values that range between −71.52 and −75.04 kcal mol^{-1} which are slightly less. The remaining quantities ($S°$, $\Delta S_f°$, etc.) also vary with the degree of branching whose behavior becomes apparent by inspection and is omitted for brevity.

The ideal gas heat capacity data given in Tables XVII and XVIII were used to determine the constants in the following polynomial form by least squares

$$C_p° = a_0 + a_1T + a_2T^2 + a_3T^3 + a_4/T^2 \qquad (24)$$

Values for the constants a_0, a_1, ..., a_4 are given in Table XIX for the C_{14} enals and Table XX for the C_{16} amines. The percent root mean square deviation between the estimated and fitted values for $C_p°$ never exceeded 0.1%. The heat capacity data given in Tables XVII and XVIII can be used to identify the constants in other equations forms, but eq 24 was found to give superior results when compared to others having the same or a lesser number of constants.

Liquid Heat Capacities. The experimental liquid heat capacity for each compound listed in Table V is given in Tables XXI–XXIII along with the relative errors obtained when various corresponding-state methods were used to estimate the liquid heat capacities. The specific ones used here include the Rowlinson correlation (*21*) as modified by Bondi (*22*), the Sternling and Brown correlation (*22*), and the Yuan and Stiel correlation (*23*) as applied to nonpolar liquids. These are given

Table XVII. Ideal Gas Enthalpy of Formation, Entropy, Entropy of Formation, Free Energy of Formation, and Heat Capacity for C_{14} Unsaturated Aldehydes

index	compound	ΔH_f°, kcal mol^{-1}	S°, cal mol^{-1} K^{-1}	ΔS_f°,[a] cal mol^{-1} K^{-1}	ΔG_f°,[b] kcal mol^{-1}	C_p°, cal mol^{-1} K^{-1} 300 K	400 K	500 K	600 K	800 K	1000 K
1	2-(3-MeBu)-5-MeOctenal	−77.80	188.09	−262.48	0.460	72.82	93.13	111.36	126.65	150.33	167.66
2	2-(1-MeBu)-5-MeOctenal	−75.57	189.45	−262.12	2.282	70.14	90.95	109.84	125.43	149.55	167.14
3	2-Pe-5-MeOctenal	−76.52	190.77	−259.80	0.940	73.09	93.19	111.29	126.51	150.14	167.52
4	2-(3-MeBu)-7-MeOctenal	−74.84	176.91	−273.66	6.752	69.04	87.36	103.85	117.77	139.50	155.44
5	2-PeNonenal	−77.04	192.07	−258.50	0.030	74.70	94.34	112.03	126.98	150.34	167.64
6	2-Pe-7-MeOctenal	−78.32	189.39	−261.18	−0.450	74.43	94.28	112.10	127.12	150.53	167.78
7	2-(3-MeBu)-Nonenal	−78.32	189.39	−261.18	−0.450	74.43	94.28	112.10	127.12	150.53	167.78
8	2-(1-MeBu)-7-MeOctenal	−78.37	188.08	−262.49	−0.107	72.82	93.13	111.46	126.65	150.33	167.66
9	2-Pe-4-MeOctenal	−77.09	190.76	−259.81	0.373	73.09	93.19	111.39	126.51	150.14	167.52
10	2-(3-MeBu)-4-MeOctenal	−78.37	188.08	−262.49	−0.107	72.82	93.13	111.46	126.65	150.33	167.66
11	2-(1-MeBu)-Nonenal	−77.09	190.76	−259.81	0.373	73.09	93.19	111.39	126.51	150.14	167.52
12	2-Pe-4-EtHeptenal	−76.29	190.76	−259.81	1.173	73.09	93.19	111.39	126.51	150.14	167.52
13	2-(3-MeBu)-4-EtHeptenal	−77.57	188.08	−262.49	0.693	72.82	93.13	111.46	126.65	150.33	167.66
14	2-(1-MeBu)-4-MeOctenal	−76.14	189.44	−261.13	1.715	70.14	90.95	109.94	125.43	149.55	167.14
15	2-(1-MeBu)-4-EtHeptenal	−75.34	189.44	−261.13	2.515	70.14	90.95	109.94	125.43	149.55	167.14
16	2-(1,2-DiMePr)-5,6-DiMeHeptenal	−78.13	184.09	−266.58	1.322	69.60	90.83	109.98	125.71	149.93	167.42
17	2-Pe-5,6-DiMeHeptenal	−77.80	188.09	−262.48	0.460	72.72	93.13	111.36	126.65	150.33	167.66
18	2-(1,2-DiMePr)-Nonenal	−78.37	188.08	−262.49	−0.107	72.82	93.13	111.46	126.65	150.33	167.66
19	2-(3-MeBu)-5,6-DiMeHeptenal	−79.08	185.40	−265.17	−0.020	72.55	93.07	111.43	126.79	150.52	167.80
20	2-(1,2-DiMePr)-7-MeOctenal	−79.65	185.39	−265.18	−0.588	72.55	93.07	111.53	126.79	150.52	167.80
21	2-(1,2-DiMePr)-5-MeOctenal	−76.85	186.77	−263.80	1.802	69.87	90.89	109.91	125.57	149.74	167.28
22	2-(1-MeBu)-5,6-DiMeHeptenal	−76.85	186.77	−263.80	1.802	69.87	90.89	109.91	125.57	149.74	167.28
23	2-(1,2-DiMePr)-4-MeOctenal	−77.42	186.76	−263.81	1.235	69.87	90.89	109.91	125.57	149.74	167.28
24	2-(1,2-DiMePr)-4-EtHeptenal	−76.62	186.76	−263.81	2.035	69.87	90.89	109.91	125.57	149.74	167.28
25	2-Pe-4,6-DiMeHeptenal	−78.37	188.08	−262.49	−0.107	72.82	93.13	111.46	126.65	150.33	167.66
26	2-(3-MeBu)-4,6-DiMeHeptenal	−79.65	185.39	−265.18	−0.588	72.55	93.07	111.53	126.79	150.52	167.80
27	2-(1,2-DiMePr)-4,6-DiHeptenal	−78.70	184.08	−266.79	0.755	69.60	90.83	110.08	125.71	149.93	167.42
28	2-(1-MeBu)-4,6-DiMeHeptenal	−77.42	186.76	−263.81	1.235	69.87	90.89	110.01	125.57	149.74	167.28

[a] $\Delta S_f^\circ = S^\circ - \sum_{i=1}^{n}\nu_{e,i}S_{e,i}^\circ$. [b] $\Delta G_f^\circ = \Delta H_f^\circ = T\Delta S_f^\circ$.

by eq 25–28 in terms of of the ideal gas heat capacity C_p° and the acentric factor ω.

Rowlinson correlation

$$C_{pL} = C_p^\circ + R\{2.56 + 0.436(1 - T_r)^{-1} + \omega[2.91 + 4.28(1 - T_r)^{1/3}T_r^{-1} + 0.296(1 - T_r)^{-1}]\} \quad (25)$$

Sternling and Brown correlation

$$C_{pL} = C_p^\circ + R\{(0.5 + 2.2\omega)[3.67 + 11.64(1 - T_r)^4 + 0.634(1 - T_r)^{-1}]\} \quad (26)$$

Yuan and Stiel correlation

$$C_{pL} = C_{\sigma L} + R\{(1 + \omega)^{0.85} \exp(-0.7074 - 31.014T_r + 34.361T_r^2)\} \quad (27)$$

where

$$C_{\sigma L} = C_p^\circ + (\Delta C_\sigma)^{(0)} + \omega(\Delta C_\sigma)^{(1)} \quad (28)$$

Values for the deviation functions $(\Delta C_\sigma)^{(0)}$ and $(\Delta C_\sigma)^{(1)}$ are tabulated in Reid et al. (*5*) as a function of reduced temperature. The experimental data were also fitted by least squares to various empirical equations. The following polynomial form was found to give good results:

$$C_{pL} = a_0 + a_1T + a_2T^2 \quad (29)$$

The results given in Tables XXI–XXIII show that the various corresponding-states correlations generally underpredict the experimental values with a worst case mean deviation not greater than 6.5% which is quite satisfactory for engineering purposes. Among the various correlations, the Yuan and Stiel correlation (*23*) has less error at the lower temperatures, but this advantage decreases at the higher temperatures. The empirical equations gives the least error, but this form cannot be used for predictive purposes for the remaining novel compounds where data is currently lacking.

Summary and Conclusions

Normal boiling temperatures, critical constants, vapor pressures, liquid densities, liquid heat capacities, and various ideal gas thermodynamic properties have been obtained for 28 branched isomeric C_{14} unsaturated aldehydes and 28 branched isomeric C_{16} saturated amines. Experimental measurements of certain key properties for the least and highly branched members of this group of novel compounds were compared to results obtained from various group contribution and used to identify parameters in assorted correlating equations.

It was shown that the Miller vapor pressure equation gave the lowest errors when compared to the Antoine and Riedel–Plank–Miller vapor pressure equations. Of these various equations, only the constants in the Riedel–Plank–Miller equations can be developed by using group contribution techniques which is useful for novel compounds. The relative errors between the experimental and predicted values for the vapor pressures for this latter equation were significantly larger than for either the Miller or the Antoine equations. This was attributed to errors in the estimated values for the critical pressure and critical temperature that were previously derived by using Lydersen's method.

Extrapolation of the vapor pressure data by unconstrained fitting of the Riedel–Plank–Miller equation and two other vapor pressure equations that are based upon corresponding-states principles was used to develop independent estimates of the critical pressure, critical temperature, and the acentric factor. While all three equations produce good fits with the data, the values for these three parameters that were obtained by the fitting procedure were somewhat inconsistent when compared to each other. One of the corresponding-states vapor pressure equation that was based upon two user-specified reference

Table XVIII. Ideal Gas Enthalpy of Formation, Entropy of Formation, Gibbs Free Energy of Formation, and Heat Capacity for Branched C_{16} Saturated Amines

index	compound	ΔH_f°, kcal mol^{-1}	S°, cal mol^{-1} K^{-1}	ΔS_f°,[a] cal mol^{-1} K^{-1}	ΔG_f°,[b] kcal mol^{-1}	C_p°, cal mol^{-1} K^{-1}					
						300 K	400 K	500 K	600 K	800 K	1000 K
1	*N*,*N*-DiMe-2-(3-MeBu)-5-MeOcAm	−73.28	187.39	−403.46	47.01	92.49	118.20	141.12	160.35	190.12	211.82
2	*N*,*N*-DiMe-2-(1-MeBu)-5-MeOcAm	−72.48	188.77	−402.08	47.40	92.49	118.20	141.12	160.35	190.12	211.82
3	*N*,*N*-DiMe-2-Pe-5-MeOcAm	−72.00	190.07	−400.78	47.44	92.76	118.26	141.05	160.21	189.93	211.63
4	*N*,*N*-DiMe-2-(3-MeBu)-7-MeOcAm	−74.08	186.01	−404.84	46.62	92.49	118.20	141.12	160.35	190.12	211.82
5	*N*,*N*-DiMe-2-PeNyAm	−71.52	191.38	−399.47	47.58	93.03	118.32	140.98	160.07	189.74	211.54
6	*N*,*N*-DiMe-2-Pe-7-MeOcAm	−72.80	188.70	−402.15	47.10	92.76	118.26	141.05	160.21	189.93	211.68
7	*N*,*N*-DiMe-2-(3-MeBu)-NyAm	−72.80	188.70	−402.15	47.10	92.76	188.26	141.05	160.21	189.93	211.68
8	*N*,*N*-DiMe-2-(1-MeBu)-7-MeOcAm	−73.28	187.39	−403.46	47.01	92.49	118.20	141.12	160.35	190.12	211.82
9	*N*,*N*-DiMe-2-Pe-4-MeOcAm	−72.80	190.07	−400.78	46.69	92.76	118.26	141.05	160.21	189.93	211.68
10	*N*,*N*-DiMe-2-(3-MeBu)-4-MeOcAm	−73.28	187.39	−403.46	47.01	92.49	118.20	141.12	160.35	190.12	211.82
11	*N*,*N*-DiMe-2-(1-MeBu)-NyAm	−72.00	190.07	−400.78	47.44	92.76	118.26	141.05	160.21	189.93	211.68
12	*N*,*N*-DiMe-2-Pe-4-EtHeAm	−71.20	190.07	−400.78	48.29	92.76	118.26	141.05	160.21	189.93	211.68
13	*N*,*N*-DiMe-2-(3-MeBu)-4-EtHpAm	−72.48	187.39	−403.46	47.81	92.49	118.20	141.12	160.35	190.12	211.82
14	*N*,*N*-DiMe-2-(1-MeBu)-4-MeOcAm	−72.48	188.77	−402.08	47.40	92.49	118.20	141.12	160.35	190.12	211.82
15	*N*,*N*-DiMe-2-(1-MeBu)-4-EtHpAm	−71.68	188.77	−402.08	48.20	92.49	118.20	141.12	160.35	190.12	211.82
16	*N*,*N*-DiMe-2-(1,2-DiMePr)-5,6-DiMeHpAm	−75.04	183.40	−407.45	46.44	91.95	118.08	141.26	160.63	190.50	212.10
17	*N*,*N*-DiMe-2-Pe-5,6-DiMeHpAm	−73.28	187.39	−403.46	47.01	92.49	118.20	114.12	160.35	190.12	211.82
18	*N*,*N*-DiMe-2-(1,2-DiMePr)-NyAm	−73.28	187.39	−403.46	47.01	92.49	118.20	141.12	160.35	190.12	211.82
19	*N*,*N*-DiMe-2-(3-MeBu)-5,6-DiMeHpAm	−74.5	184.71	−406.14	46.53	92.22	118.14	141.19	160.49	190.31	211.96
20	*N*,*N*-DiMe-2-(1,2-DiMePr)-7-MeOcAm	−74.5	184.71	−406.14	46.53	92.22	118.14	141.19	160.49	190.31	211.96
21	*N*,*N*-DiMe-2-(1,2-DiMePr)-5-MeOcAm	−73.76	186.08	−404.77	46.92	92.22	118.14	141.19	160.49	190.31	211.96
22	*N*,*N*-DiMe-2-(1-MeBu)-5,6-DiMeHpAm	−73.76	186.08	−404.77	46.92	92.22	118.14	141.19	160.49	190.31	211.96
23	*N*,*N*-DiMe-2-(1,2-DiMePr)-4-MeOcAm	−73.76	186.08	−404.77	46.92	92.22	118.14	141.19	160.49	190.31	211.96
24	*N*,*N*-DiMe-2-(1,2-DiMePr)-4-EtHpAm	−72.96	186.08	−404.77	47.92	92.22	118.14	141.19	160.49	190.31	211.96
25	*N*,*N*-DiMe-2-Pe-4,6-DiMeHpAm	−73.28	187.39	−403.46	47.01	92.49	118.20	141.12	160.35	190.12	211.82
26	*N*,*N*-DiMe-2-(3-MeBu)-4,6-DiMeHpAm	−74.5	184.71	−406.14	46.53	92.22	118.14	141.19	160.49	190.31	211.96
27	*N*,*N*-DiMe-2-(1,2-DiMePr)-4,6-DiMeHpAm	−45.04	183.40	−407.45	46.44	91.95	118.08	141.26	160.63	190.50	212.10
28	*N*,*N*-DiMe-2-(1-MeBu)-4,6-DiMeHpAm	−73.76	186.08	−404.77	46.92	92.22	118.14	141.19	160.49	190.31	211.96

[a] $\Delta S_f^\circ = S^\circ - \sum_{i=1}^{n} \nu_{e,i} S_{e,i}^\circ$. [b] $\Delta G_f^\circ = \Delta H_f^\circ - T\Delta S_f^\circ$.

Table XIX. Ideal Gas Heat Capacity Polynomial Constants for C_{14} Unsaturated Aldehydes

compound	$-10^{-2}a_0$	a_1	$-10^{3}a_2$	$10^{7}a_3$	$10^{-6}a_4$
2-(3-MeBu)-5-MeOctenal	0.385 768	0.433 218	0.330 236	0.102 505	0.754 497
2-(1-MeBu)-5-MeOctenal	0.528 298	0.476 485	0.379 297	0.121 814	0.978 174
2-Pe-5-MeOctenal	0.378 923	0.430 436	0.327 654	0.101 862	0.772 945
2-(3-MeBu)-7-MeOctenal	0.290 141	0.379 949	0.281 594	0.085 464	0.639 335
2-PeNonenal	0.313 996	0.411 151	0.307 374	0.094 559	0.707 702
2-Pe-7-MeOctenal	0.320 847	0.413 934	0.309 958	0.095 204	0.689 269
2-(3-MeBu)-Nonenal	0.320 847	0.413 934	0.309 958	0.095 204	0.689 269
2-(1-MeBu)-7-MeOctenal	0.411 579	0.443 277	0.343 647	0.108 389	0.809 395
2-Pe-4-MeOctenal	0.404 678	0.440 476	0.341 042	0.107 735	0.827 699
2-(3-MeBu)-4-MeOctenal	0.411 579	0.443 277	0.343 647	0.108 389	0.809 395
2-(1-MeBu)-Nonenal	0.404 678	0.440 476	0.341 042	0.107 735	0.827 699
2-Pe-4-EtHeptenal	0.404 678	0.440 476	0.341 042	0.107 735	0.827 699
2-(3-MeBu)-4-EtHeptenal	0.411 579	0.443 277	0.343 647	0.108 289	0.809 395
2-(1-MeBu)-4-MeOctenal	0.554 504	0.486 685	0.392 887	0.127 772	1.034 082
2-(1-MeBu)-4-EtHeptenal	0.554 504	0.486 685	0.392 887	0.127 772	1.034 082
2-(1,2-DiMePr)-5,6-DiMeHeptenal	0.542 197	0.482 122	0.384 553	0.123 139	0.941 813
2-Pe-5,6-DiMeHeptenal	0.385 768	0.433 218	0.330 236	0.102 505	0.754 497
2-(1,2-DiMePr)-Nonenal	0.411 579	0.443 277	0.343 647	0.108 389	0.809 395
2-(3-MeBu)-5,6-DiMeHeptenal	0.392 644	0.436 010	0.332 831	0.103 154	0.736 128
2-(1,2-DiMePr)-7-MeOctenal	0.418 497	0.446 084	0.346 261	0.109 045	0.791 136
2-(1,2-DiMePr)-5-MeOctenal	0.535 247	0.479 303	0.281 925	0.122 476	0.959 991
2-(1-MeBu)-5,6-DiMeHeptenal	0.535 247	0.479 303	0.381 925	0.122 476	0.959 991
2-(1,2-DiMePr)-4-MeOctenal	0.561 488	0.489 516	0.395 529	0.128 441	1.015 994
2-(1,2-DiMePr)-4-EtHeptenal	0.561 488	0.489 516	0.395 529	0.128 441	1.015 994
2-Pe-4,6-DiMeHeptenal	0.411 579	0.443 277	0.343 647	0.108 389	0.809 395
2-(3-MeBu)-4,6-DiMeHeptenal	0.418 497	0.446 084	0.346 261	0.109 045	0.791 136
2-(1,2-DiMePr)-4,6-DiMeHeptenal	0.568 482	0.492 350	0.398 177	0.129 112	0.997 927
2-(1-MeBu)-4,6-DiMeHeptenal	0.561 488	0.489 516	0.395 529	0.128 441	1.015 994

fluids produced values for the critical pressure and critical temperature that more closely approached the same parameters derived from Lydersen's group contribution method. These values for the critical pressure and critical temperature appear to be more probable since they are similar in magnitude to those for related compounds of nearly the same type and structure. Additional high-quality vapor pressure data that span a larger temperature range where the compounds of this study are known to be stable are needed for more accurate extrapolations and evaluation of critical properties.

Correlation and prediction of liquid density data showed that an empirical equation form containing two adjustable constants gave errors of less than 1%. The Yen–Woods equation gave acceptable errors of less than 5% when constants based upon group contribution techniques were used.

Various ideal gas thermodynamic properties such as ideal gas enthalpy of formation, entropy, entropy of formation, Gibbs free energy of formation, and heat capacity were derived for

Table XX. Ideal Gas Heat Capacity Polynomial Constants for C_{16} Saturated Amines

compound	$-10^{-2}a_0$	a_1	-10^3a_2	10^6a_3	$10^{-6}a_4$
N,*N*-DiMe-2-(3-MeBu)-5-MeOcAm	0.424 418	0.527 771	0.394 300	0.119 998	0.795 823
N,*N*-DiMe-2-(1-MeBu)-5-MeOcAm	0.424 418	0.527 771	0.394 300	0.119 998	0.795 823
N,*N*-DiMe-2-Pe-5-MeOcAm	0.418 209	0.525 219	0.392 008	0.119 477	0.815 877
N,*N*-DiMe-2-(3-MeBu)-7-MeOcAm	0.424 418	0.527 771	0.394 300	0.119 998	0.795 823
N,*N*-DiMe-2-PeNyAm	0.412 000	0.522 666	0.389 716	0.118 956	0.835 930
N,*N*-DiMe-2-Pe-7-MeOcAm	0.418 209	0.525 219	0.392 006	0.119 477	0.815 877
N,*N*-DiMe-2-(3-MeBu)-NyAm	0.418 209	0.525 219	0.392 008	0.119 477	0.815 877
N,*N*-DiMe-2-(1-MeBu)-7-MeOcAm	0.424 418	0.527 771	0.394 300	0.119 998	0.795 823
N,*N*-DiMe-2-Pe-4-MeOcAm	0.418 209	0.525 219	0.392 008	0.119 477	0.815 877
N,*N*-DiMe-2-(3-MeBu)-4-MeOcAm	0.424 418	0.527 771	0.394 300	0.119 998	0.795 823
N,*N*-DiMe-2-(1-MeBu)-NyAm	0.418 209	0.525 219	0.392 008	0.119 477	0.815 877
N,*N*-DiMe-2-Pe-4-EtHpAm	0.418 209	0.525 219	0.392 008	0.119 477	0.815 877
N,*N*-DiMe-2-(3-MeBu)-4-EtHpAm	0.424 418	0.527 771	0.394 300	0.119 998	0.795 823
N,*N*-DiMe-2-(1-MeBu)-4-MeOcAm	0.424 418	0.527 771	0.394 300	0.119 998	0.795 823
N,*N*-DiMe-2-(1-MeBu)-4-EtHpAm	0.424 418	0.527 771	0.364 300	0.119 998	0.795 823
N,*N*-DiMe-2-(1,2-DiMePr)-5,6-DiMeHpAm	0.436 836	0.532 876	0.398 884	0.121 039	0.755 716
N,*N*-DiMe-2-Pe-5,6-DiMeHpAm	0.424 418	0.527 771	0.394 300	0.119 998	0.795 823
N,*N*-DiMe-2-(1,2-DiMePr)-NyAm	0.424 418	0.527 771	0.394 300	0.119 998	0.795 823
N,*N*-DiMe-2-(3-MeBu)-5,6-DiMeHpAm	0.430 627	0.530 324	0.396 592	0.120 518	0.775 769
N,*N*-DiMe-2-(1,2-DiMePr)-7-MeOcAm	0.430 627	0.530 324	0.396 592	0.120 518	0.775 769
N,*N*-DiMe-2-(1,2-DiMePr)-5-MeOcAm	0.430 627	0.530 324	0.396 592	0.120 518	0.775 769
N,*N*-DiMe-2-(1-MeBu)-5,6-DiMeHpAm	0.430 627	0.530 324	0.396 592	0.120 518	0.775 769
N,*N*-DiMe-2-(1,2-DiMePr)-4-MeOcAm	0.430 627	0.530 324	0.396 592	0.120 518	0.775 769
N,*N*-DiMe-2-(1,2-DiMePr)-4-EtHpAm	0.430 627	0.530 324	0.396 592	0.120 518	0.775 769
N,*N*-DiMe-2-Pe-4,6-DiMeHpAm	0.424 418	0.527 771	0.394 300	0.119 998	0.795 823
N,*N*-DiMe-2-(3-MeBu)-4,6-DiMeHpAm	0.430 627	0.530 324	0.396 592	0.120 518	0.775 769
N,*N*-DiMe-2-(1,2-DiMePr)-4,6-DiMeHpAm	0.436 836	0.532 876	0.398 884	0.121 039	0.755 716
N,*N*-DiMe-2-(1-MeBu)-4,6-DiMeHpAm	0.430 627	0.530 324	0.396 592	0.120 518	0.775 769

Table XXI. Liquid Heat Capacities of 2-Pentylnonenal

obsd		ϵ^e			
T, K	C_{pL}, cal mol^{-1} K^{-1}	Bondi eq[a]	Sternling–Brown eq[b]	Yuan–Stiel eq[c]	empirical[d]
323.15	104.05	3.42	2.23	−1.91	0.72
328.15	104.19	2.78	1.58	−2.37	0.19
333.15	105.27	3.00	1.80	−1.92	0.51
338.15	105.58	2.52	1.31	−2.21	0.07
343.15	106.65	2.73	1.52	−1.78	0.31
348.15	106.97	2.25	1.02	−2.08	−0.19
353.15	107.73	2.17	0.92	−1.96	−0.32
358.15	108.51	2.10	0.85	−1.83	−0.46
363.15	109.12	1.89	0.61	−1.86	−0.79
368.15	108.82	0.86	−0.45	−2.73	−1.99
373.15	110.50	1.62	0.29	−1.77	−1.38
378.15	111.74	1.96	0.62	−1.23	−1.23
383.15	114.21	3.35	2.00	0.37	−0.04
388.15	116.67	4.67	3.31	1.90	1.07
393.15	118.06	5.09	3.71	2.49	1.21
398.15	119.28	5.36	3.95	2.93	1.18
403.15	121.44	6.36	4.94	4.09	1.88
408.15	122.20	6.26	4.80	4.12	1.41
413.15	122.37	5.71	4.20	3.69	0.43
418.15	123.13	5.62	4.07	3.70	−0.09
423.15	123.27	5.06	3.46	3.24	−1.14
428.15	124.20	5.11	3.46	3.39	−1.58

	Bondi eq	Sternling–Brown eq	Yuan–Stiel eq	empirical
mean dev[f]	3.63	2.32	2.44	0.83
max dev[e]	6.36	4.94	4.12	−1.99

[a] From eq 25. [b] From eq 26. [c] From eq 27. [d] From eq 29. [e] ϵ = heat capacity deviation= $100(C_{pL,exptl} - C_{pL,calcd})/C_{pL,exptl}$. [f] $100\sum_i(|C_{pL,exptl} - C_{pL,calcd}|/C_{pL,exptl})_i/n$.

Table XXII. Liquid Heat Capacities of 2-(1,2-Dimethylpropyl)-5,6-dimethylheptenal

obsd		ϵ^e			
T, K	C_{pL}, cal mol^{-1} K^{-1}	Bondi eq[a]	Sternling–Brown eq[b]	Yuan–Stiel eq[c]	empirical[d]
323.15	100.15	4.04	3.29	0.50	0.35
328.15	101.06	4.01	3.27	0.63	0.38
333.15	102.17	4.17	3.45	0.95	0.59
338.15	102.64	3.72	3.00	0.65	0.15
343.15	102.64	2.84	2.12	−0.11	−0.75
348.15	103.75	3.00	2.29	0.22	−0.59
353.15	104.66	2.98	2.26	0.34	−0.65
358.15	106.00	3.35	2.64	0.86	−0.30
363.15	107.12	3.51	2.79	1.17	−0.20
368.15	108.02	3.48	2.76	1.27	−0.32
373.15	108.90	3.43	2.70	1.35	−0.47
378.15	110.48	3.99	3.25	2.05	−0.01
383.15	112.50	4.91	4.17	3.12	0.82
388.15	113.18	4.68	3.92	3.00	0.43
393.15	114.52	5.02	4.24	3.47	0.61
398.15	115.66	5.18	4.38	3.74	0.59
403.15	116.33	4.96	4.14	3.61	0.16
408.15	117.21	4.91	4.07	3.66	−0.11
413.15	118.35	5.07	4.21	3.92	−0.17
418.15	119.70	5.40	4.51	4.33	−0.07
423.15	121.04	5.72	4.81	4.73	0.00
428.15	121.72	5.52	4.58	4.60	−0.49

	Bondi eq	Sternling–Brown eq	Yuan–Stiel eq	empirical eq
mean dev[f]	4.27	3.49	2.19	0.37
max dev[e]	5.72	4.81	4.73	0.82

[a] From eq 25. [b] From eq 26. [c] From eq 27. [d] From eq 29. [e] ϵ = heat capacity deviation = $100(C_{pL,exptl} - C_{pL,calcd})/C_{pL,exptl}$. [f] $100\sum_i(|C_{pL,exptl} - C_{pL,calcd}|/C_{pL,exptl})_i/n$.

all 56 compounds by using Benson's method. Constants for a ideal gas heat capacity polynomial were determined for each compound and produced predicted values having a percent root mean square deviation of less than 0.1% when compared to the Benson group contribution based values.

Liquid heat capacity data were compared to predictions derived from the Rowlinson, Sternling and Brown, and Yuan and Stiel generalized correlations. In addition, the data were fitted to an empirical polynomial form that was quadratic in absolute temperature. The mean deviations for all three generalized correlations did not exceed 6.5%, with those for the Yuan and Stiel correlations being slightly less. The empirical form had a mean deviation of less than 1%, but the constants correspond to a specific compound and cannot be used for predictions involving novel compounds where data are not yet available.

Table XXIII. Liquid Heat Capacities of *N*,*N*-Dimethyl-2-pentylnonylamine

obsd		ϵ^e			
T, K	C_{pL}, cal mol^{-1} K^{-1}	Bondi eq[a]	Sternling–Brown eq[b]	Yuan–Stiel eq[c]	empirical[d]
323.15	128.58	7.63	6.74	3.71	0.42
328.15	129.76	7.60	6.71	3.84	0.48
333.15	130.27	7.08	6.18	3.48	0.01
338.15	130.92	6.66	5.76	3.22	−0.35
343.15	132.76	7.09	6.19	3.82	0.19
348.15	134.04	7.12	6.21	4.01	0.30
353.15	134.83	6.81	5.90	3.85	0.04
358.15	131.89	3.86	2.91	0.96	−3.07
363.15	137.18	6.73	5.79	4.07	0.06
368.15	138.48	6.78	5.83	4.26	0.15
373.15	139.64	6.74	5.77	4.35	0.14
378.15	140.80	6.69	5.71	4.44	0.12
383.15	142.49	7.00	6.00	4.89	0.47
388.15	143.94	7.14	6.12	5.16	0.64
393.15	144.71	6.85	5.81	5.00	0.33
398.15	146.52	7.23	6.17	5.49	0.73
403.15	146.93	6.73	5.63	5.08	0.18
408.15	147.56	6.36	5.23	4.81	−0.24
413.15	149.39	6.76	5.61	5.31	0.17
418.15	149.78	6.25	5.06	4.88	−0.41
423.15	150.94	6.24	5.01	4.95	−0.47

	Bondi eq	Sternling–Brown eq	Yuan–Stiel eq	empirical eq
mean dev[f]	6.45	5.73	4.27	0.43
max dev[e]	7.63	6.74	5.49	−3.07

[a] From eq 25. [b] From eq 26. [c] From eq 27. [d] From eq 29. [e] ϵ = heat capacity deviation= $100(C_{pL,\mathrm{exptl}} - C_{pL,\mathrm{calcd}})/C_{pL,\mathrm{exptl}}$. [f] $100\sum_i (|C_{pL,\mathrm{exptl}} - C_{pL,\mathrm{calcd}}|/C_{pL,\mathrm{exptl}})_i/n$.

Acknowledgment

We acknowledge Frank J. Doering, Mark Trampe, and A. J. Solodar for their efforts in preparing the compounds. In addition, we acknowledge the Physical Sciences Center for making the experimental physical property measurements.

Glossary

a_j	ideal gas heat capacity polynomial constants in eq 24
A	liquid density constant in eq 20
A_a	Antoine vapor pressure equation constant in eq 4
A_m	Miller vapor pressure equation constant in eq 3
b_j	Yen–Woods equation constants in eq 20
B	liquid density constant in eq 20
B_a	Antoine vapor pressure equation constant in eq 4
B_m	Miller vapor pressure equation constant in eq 3
C_a	Antoine vapor pressure equation constant in eq 4
C_m	Miller vapor pressure equation constant in eq 3
$C_p{}^\circ$	ideal gas heat capacity, cal mol^{-1} K^{-1}
C_{pL}	liquid heat capacity at constant pressure, cal mol^{-1} K^{-1}
$C_{\sigma L}$	saturated liquid heat capacity, cal mol^{-1} K^{-1}
D_a	Antoine vapor pressure equation constant defined by eq 7
D_m	Miller vapor pressure equation constant in eq 3
G	Riedel-Plank-Miller vapor pressure equation constant defined by eq 9
$\Delta G_f{}^\circ$	standard Gibbs energy of formation defined by eq 23, cal mol^{-1}
h	Riedel–Plank–Miller vapor pressure equation constant defined by eq 8
$\Delta H_f{}^\circ$	standard enthalpy of formation, cal mol^{-1} K^{-1}
k	Riedel–Plank–Miller vapor pressure equation constant defined by eq 10
K_j	Yen–Wood saturated liquid density equation constant in eq 18
n	denotes the total number of points
P	vapor pressure, kPa
P_c	critical pressure, atm or kPa
P_r	reduced vapor pressure in eq 11, dimensionless
R	ideal gas constant, J K^{-1} mol^{-1}
$S^\circ{}_{298}$	ideal gas entropy, cal mol^{-1} K^{-1}
$\Delta S_f{}^\circ$	standard entropy of formation, cal mol^{-1} K^{-1}
T	temperature, K
T_b	normal boiling temperature in eq 1, K
T_{br}	reduced normal boiling temperature in eq 1, dimensionless
T_c	critical temperature in eq 1, K
T_r	reduced temperature, T/T_c, dimensionless
$T_{r,\mathrm{ref}}$	reduced temperature at the reference temperature, dimensionless
V_c	critical volume, cm^3 mol^{-1}
Z_c	critical compressibility, dimensionless

Greek Letters

ϵ	percent deviation in Table V
ρ_c	critical density in eq 18, g cm^{-3}
ρ_{ref}	saturated liquid density at the reference temperature in eq 19, g cm^{-3}
ρ_s	saturated liquid density at the solution temperature T in eq 18, g cm^{-3}
ω	acentric factor defined by eq 15, dimensionless

Literature Cited

(1) Forster, D.; Schaefer, G. F.; Barker, G. E. "New Route to Long Chain Amines"; U.S. Patent 4 598 162, 1986.
(2) Willis, D. E. *J. Chromatogr. Sci*. **1983**, *21*, 132.
(3) Mills, P. L. *J. Chem. Eng. Data*, preceding paper in this issue.
(4) Fedors, R. F. *Chem. Eng. Commun*. **1982**, *16*, 149.
(5) Reid, R. C.; Prausnitz, J. M.; Sherwood, T. K. *The Properties of Gases and Liquids*, 3rd ed.; McGraw-Hill: New York, 1977.
(6) Watson, K. M. *Ind. Eng. Chem*. **1931**, *23*, 360.
(7) Miller, D. G. *Ind. Eng. Chem*. **1964**, *56*, 46.
(8) Antoine, C. *Chem. Rev*. **1888**, *107*, 681.
(9) Miller, D. G. *J. Phys. Chem*. **1965**, *69*, 3209.
(10) Ambrose, D. *J. Chem. Thermodyn*. **1978**, *10*, 765.
(11) Ambrose, D.; Counsel, J. F.; Hicks, C. P. *J. Chem. Thermodyn*. **1978**, *10*, 771.
(12) Ambrose, D.; Patel, N. C. *J. Chem. Thermodyn*. **1984**, *16*, 459.
(13) Lee, B. I.; Kesler, M. G. *AIChE J*. **1975**, *21*, 510.
(14) Wagner, W. *Bull. Inst, Froid Annexe* **1973**, *4*, 65.
(15) Wagner, W.; Ewers, J.; Pentermann, W. *J. Chem. Thermodyn*. **1976**, *8*, 1049.
(16) Marquardt, D. W. *J. Soc. Ind. Appl. Math*. **1963**, *11*, 431.
(17) Yen, L. C.; Woods, S. S. *AIChE J*. **1966**, *12*, 95.
(18) Benson, S. W. *Thermochemical Kinetics*; Wiley: New York, 1968.
(19) Benson, S. W.; Cruickshank, F. R.; Golden, D. M.; Haugen, G. R.; O'Neal, H. E.; Rudgers, A. S.; Shaw, R.; Walsh, R. *Chem. Rev*. **1969**, *69*, 279.
(20) Stull, D. R.; Westrum, Sinke, G. C. *The Chemical Thermodynamics of Organic Compounds*; Wiley: New York, 1969.
(21) Rowlinson, J. S. *Liquids and Liquid Mixtures*, 2nd ed.; Butterworth: London, 1969.
(22) Bondi, A. *Ind. Eng. Chem. Fundam*. **1966**, *5*, 443.
(23) Yuan, T. F.; Stiel, L. I. *Ind. Eng. Chem. Fundam*. **1970**, *9*, 393.

Received for review December 5, 1985. Accepted December 16, 1986.

Supplementary Material Available: Group contribution and correction terms for evaluation of C_{14} enal and C_{16} amine ideal gas properties by Benson's method (12 pages). Ordering information is given on any current masthead page.